

RESEARCH ARTICLE

The impact of oyster aquaculture on the estuarine carbonate system

Catherine M. Liberti^{1,*}, Matthew W. Gray², Lawrence M. Mayer¹, Jeremy M. Testa³, Wei Liu³, and Damian C. Brady¹

Many studies have examined the vulnerability of calcifying organisms, such as the eastern oyster (Crassostrea virginica), to externally forced ocean acidification, but the opposite interaction whereby oysters alter their local carbonate conditions has received far less attention. We present an exploratory model for isolating the impact that net calcification and respiration of aquacultured eastern oysters can have on calcite and aragonite saturation states, in the context of varying temperature, ocean-estuary mixing, and air-sea gas exchange. We apply the model to the Damariscotta River Estuary in Maine which has experienced rapid expansion of oyster aquaculture in the last decade. Our model uses oyster shell growth over the summer season and a previously derived relationship between net calcification and respiration to quantify impacts of net oyster calcification and gross metabolism on carbonate saturation states in open tidal waters. Under 2018 industry size and climate conditions, we estimate that oysters can lower carbonate saturation states by up to 5% (i.e., 0.17 and 0.11 units on calcite and aragonite saturation states, respectively) per day in late summer, with an average of 3% over the growing season. Perturbations from temperature and air-sea exchange are similar in magnitude. Under 2050 climate conditions and 2018 industry size, calcite saturation state will decrease by up to an additional 0.54 units. If the industry expands 3-fold by 2050, the calcite and aragonite saturation states may decrease by 0.73 and 0.47 units, respectively, on average for the latter half of the growing season when compared to 2018 climate conditions and industry size. Collectively, our results indicate that dense aggregations of oysters can have a significant role on estuarine carbonate chemistry.

Keywords: Carbonate chemistry, Shellfish aquaculture, Oysters, Saturation state, Ocean acidification, Carrying capacity

Introduction

Ocean and coastal acidification (OCA) affects shellfish and other calcifying organisms due to the dissolution pressure it exerts on their exoskeleton and the elevated metabolic cost of calcification (Melzner et al., 2011; Waldbusser and Salisbury, 2014; Waldbusser et al., 2015; Gledhill et al., 2015). While there is a significant body of literature demonstrating this sensitivity and discussion around potential impacts on wild and cultured shellfish from OCA, most of the focus has been on OCA resulting from various processes, particularly global carbon emissions (Feely et al., 2004; Doney et al., 2009), local freshwater runoff (Salisbury et al., 2008; Duarte et al., 2013), ecosystem metabolism (Feely et al., 2010;

Duarte et al., 2013; Wallace et al., 2014; Pacella et al., 2018; Rheuban et al., 2019), temperature changes (Salisbury and Jönsson, 2018), and upwelling (Feely et al., 2008; Hauri et al., 2009; Hauri et al., 2013; Reum et al., 2016). However, oysters are powerful ecosystem engineers that can transform their environment (Dame, 2011), including in aquaculture settings where populations are large and dense relative to the water body volume (Dumbauld et al., 2009; Coen et al., 2011). The beneficial effects of oyster aquaculture on water clarity and suspended particulate removal (Cranford et al., 2011), nutrient cycling (Kellogg et al., 2013; Kellogg et al., 2014; Lunstrum et al., 2018; Ray et al., 2019), and carbon sequestration/removal during harvest (Ahmed et al., 2017; Fodrie et al., 2017) are well known, and oysters are considered one of the most sustainable ways to provide animal protein (Ray et al., 2019; Naylor et al., 2021). Given these environmental benefits and a high demand for oysters, global and U.S. oyster aquaculture has risen rapidly over the last several decades (Naylor et al., 2021; NOAA Fisheries, 2021).

Extensive research shows that calcification and respiration in natural populations release CO₂ into the ocean and

¹ Darling Marine Center, University of Maine School of Marine Sciences, Walpole, ME, USA

²Horn Point Laboratory, University of Maryland Center for Environmental Science, Cambridge, MD, USA

³Chesapeake Biological Laboratory, University of Maryland Center for Environmental Science, Solomons, MD, USA

^{*}Corresponding author: Email: kate.liberti@maine.edu

atmosphere (Frankignoulle et al., 1995; Gattuso et al., 1995; Gattuso et al., 1999; Zeebe and Wolf-Gladrow, 2001). However, only a few studies have focused on the potential for commercial-scale shellfish aquaculture to affect the surrounding seawater carbonate system (Mistri and Munari, 2012; Munari et al., 2013; Filgueira et al., 2015; Morris and Humphreys, 2019; Li et al., 2021), particularly in the context of shellfish aquaculture lowering surrounding carbonate saturations states (Ω) and limiting its own further expansion through decreased growth rates. Additionally, a sought-after characteristic of oysters on the half shell, a large proportion of the oyster market, is a strong shell, one that is easily shucked and does not break or chip (Mizuta and Wikfors, 2019). A reduction in the shell thickness or hardness from decreased Ω would be detrimental to the quality of the product. Therefore, considering the effect of these ecosystem engineers on estuarine carbonate chemistry to ensure environmentally sustainable and profitable expansion of oyster aquaculture is important.

Dissolved inorganic carbon (DIC) and total alkalinity (TA) are two of the most commonly measured parameters of the carbonate system in marine waters. DIC is the sum of concentrations of all inorganic carbon species and includes CO_2 , carbonic acid (H_2CO_3) , bicarbonate ion (HCO_3^-) , and carbonate ion (CO_3^{2-}) . Changes in the concentration of these species can affect the DIC of the system. Photosynthesis, respiration, calcification, and dissolution are large drivers of DIC variability, particularly in coastal areas. TA is a measure of the buffering capacity of a water body defined by Dickson (1981) as:

$$\begin{split} TA &= \left[HCO_{3}^{-}\right] + 2\left[CO_{3}^{2-}\right] + \left[B(OH)_{4}^{-}\right] + \left[OH^{-}\right] \\ &+ \left[HPO_{4}^{2-}\right] + 2\left[PO_{4}^{3-}\right] + \left[SiO(OH)_{3}^{-}\right] + \left[NH_{3}\right] \\ &+ \left[HS^{-}\right] + \ldots - \left[H^{+}\right]_{F} - \left[HSO_{4}^{-}\right] - \left[HF\right] \\ &- \left[H_{3}PO_{4}\right] - \ldots \end{split}$$

(1)

where the ellipses signify weak organic acids and bases that may contribute to TA, particularly in coastal areas. TA is thus significantly affected by calcification and dissolution, as well as processes that impact nutrient concentrations.

Oysters use calcium and carbonate to build their shells via either aragonite as larvae or calcite as juveniles and adults; both are mineral forms of calcium carbonate (CaCO $_3$). The Ω of either calcite or aragonite indicates how easily that mineral form can be precipitated through physical processes or by organisms.

$$\Omega = \left[\text{Ca}^{2+} \right] \left[\text{CO}_{3}^{2-} \right] / K_{\text{sp}}', \tag{2}$$

where $[{\rm Ca}^{2+}]$ and $[{\rm CO}_3^{2-}]$ represent ion concentrations of calcium and carbonate, and $K_{\rm sp}^{'}$ is the apparent solubility product of either aragonite or calcite. Oysters directly reduce the Ω of the surrounding water via two pathways: calcification and respiration (Zeebe and Wolf-Gladrow, 2001). Shellfish build and maintain organic tissue by ingesting food (e.g., phytoplankton and detritus) and then convert some of the particulate organic carbon in the food

into soft tissue, excreting a fraction of it as organic carbon waste and respiring the rest to CO_2 . The respired CO_2 can react with surrounding water to form H_2CO_3 that lowers pH by dissociating into HCO_3^- and a free proton. Protons bond with CO_3^{2-} , reducing their concentration and lowering the saturation state of calcium carbonate (Doney et al., 2009). This process increases the DIC/TA ratio because the CO_2 addition increases DIC but not TA. The buffering capacity of the system reaches a minimum when the DIC/TA ratio ≈ 1 (Wang et al., 2013).

Calcification changes TA with a decrease of 2 moles of TA per mole of shell $CaCO_3$ formed (Lejart et al., 2012). Skeletal calcium carbonate formation removes CO_3^{2-} and therefore TA and DIC. Calcification also converts existing DIC toward a more CO_2 rich solution, lowering pH, via a reaction such as:

$$Ca^{2+} + 2HCO_3^- = CaCO_3 + H_2O + CO_2$$
 (3)

(Frankignoulle et al., 1995; Gattuso et al., 1995; Gattuso et al., 1999). Thus, both respiration and calcification produce CO_2 that lowers Ω in surrounding waters. Unlike the open ocean, many estuaries are already supersaturated with CO₂ due to elevated organic matter remineralization (Wallace et al., 2014; Cai et al., 2017), and any further addition of CO2 increases the flux from the surface water to the overlying air, which can help reduce local acidification. The resultant Ω will depend on the ability of the system to release CO₂ produced by oyster growth into the atmosphere in addition to the impact of other processes such as photosynthesis, dissolution, mixing, and nutrient cycling (Mistri and Munari, 2012; Morris and Humphreys, 2019). Unless all of the CO₂ produced by oysters is removed, the Ω will decrease relative to the initial condition (Ware et al., 1992), creating a less favorable environment for future calcification.

Scaling these organismal effects to industry level within a growing area is complex but important given the increasing role of aquaculture to supply shellfish to market, especially where cultured bivalves are highly concentrated in productive areas. Prior studies have focused on how biotic and abiotic factors affect metabolic rates and used these relationships to scale to ecosystem level energy transfer (Enquist et al., 2003); here, we simplify and focus on the aquaculture-estuarine exchange of inorganic carbon at the industry level. Specifically, the ability of oysters to change the Ω suggests that their own growth should be considered in assessing the inorganic carbon dynamics of a water body that supports oyster aquaculture.

In estuaries that fringe the Gulf of Maine, the oyster aquaculture industry has expanded rapidly. In the last 15 years, oyster aquaculture in Maine alone has grown from 2 million to nearly 14 million oysters harvested per year (**Figure 1**). A recent analysis predicted that the robust market for eastern oysters (*Crassostrea virginica*) in the Northeast United States would lead to an expansion in the annual demand from 7 million pieces (roughly half the present harvest level in Maine) to 26 million pieces in 2030 (The Hale Group, Ltd and Gulf of Maine Research Institute, 2016). The footprint of this industry has also

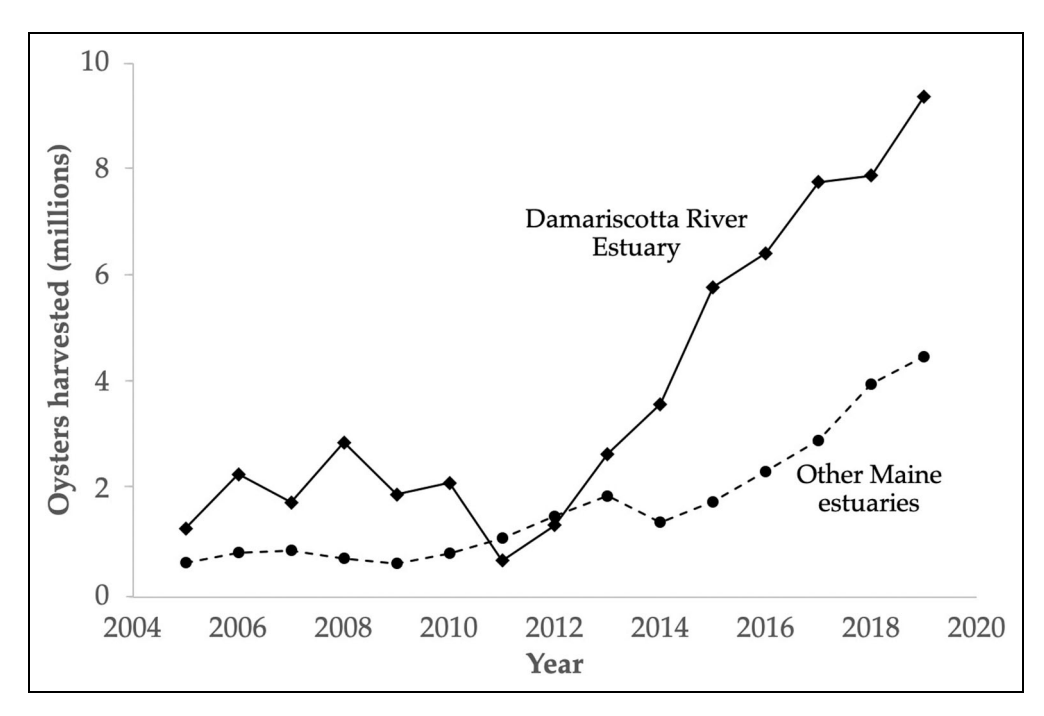


Figure 1. Cultured oyster harvest in Maine from 2005 to 2019. Cultured oyster harvest in Maine estuaries, divided into those from the Damariscotta River Estuary (black diamonds) and those from all other Maine estuaries combined (black circles). Data from Maine Department of Marine Resources, 2020. DOI: https://doi.org/10.1525/elementa.2020.00057.f1

expanded. In 2007, there were 44 active limited purpose aquaculture licenses in Maine, and in 2020 there were 769 (Maine Department of Marine Resources, 2021). Clearly the industry is growing, though not homogeneously; most growth has occurred in a few estuaries. From 2011 to 2017, the harvest from the Damariscotta River Estuary in Maine increased by 1.2 million pieces per year (Figure 1). Since 2003, when Maine Department of Marine Resources began compiling harvest data from lease and license holders, the upper Damariscotta River Estuary has consistently been the major hub for oyster aquaculture in northern New England (67% of total oyster production in Maine in 2019; Maine Department of Marine Resources, 2020). Therefore, understanding the dynamics between the industry and local estuarine conditions to enable sustainable expansion to meet the expected increase in demand is vital to the industry, local economies, and stakeholders in these communities.

In this study, we explored the potential magnitude of impact that net oyster calcification and subsequent harvest can have on estuarine carbonate chemistry to quantify whether oyster shell growth should be included as a term in carrying capacity models for shellfish. Our goal was to understand how current oyster growth might limit further industry expansion, and how future climate conditions may moderate or exacerbate the industry effect. We focused primarily on Ω_{CA} because juvenile and adult oysters predominantly use calcite to build their shells. Although we model oyster respiration, one could assume that respiration of suspended organic matter would occur in the upper Damariscotta River Estuary at similar rates regardless of whether the shellfish aquaculture industry was present or not. Therefore, our exploratory model was

primarily concerned with calculating the carbon impact of calcareous versus noncalcareous heterotrophic communities in the hydrographic conditions of the shellfish growing area.

Methods

We used the Damariscotta River Estuary oyster growing area as an example estuary because of its rapid growth in oyster aquaculture. We modeled varying industry sizes, estuarine residence times, and future OCA conditions to determine the current potential effects and how these may change in the future with industry expansion and climate change. We assumed that oyster growth was fueled by external sources of calcium, DIC, and particulate organic matter. Oysters transformed these nutrients into CaCO₃, oyster particulate organic matter (i.e., tissue), and CO₂. The CaCO₃ and oyster tissue were permanently removed from the model domain during harvest. The waste CO₂, a byproduct of CaCO₃ precipitation and metabolism, either remained in the water or was removed via oceanic exchange or air-sea exchange. CO2 that remained in the water reduced local Ω , potentially hindering future shellfish growth.

Environmental conditions

The growing area (**Figure 2**) is highly productive because of the relatively long residence time and shallow depth (average 5.5 m) that incubates Gulf of Maine water, increasing its temperatures during the growing season (6.5°C above water at the mouth of the estuary during peak temperatures) and retaining nutrients and particles such as phytoplankton (Mayer et al., 1996; Lieberthal et al., 2019; Newell et al., 2021). The Gulf of Maine

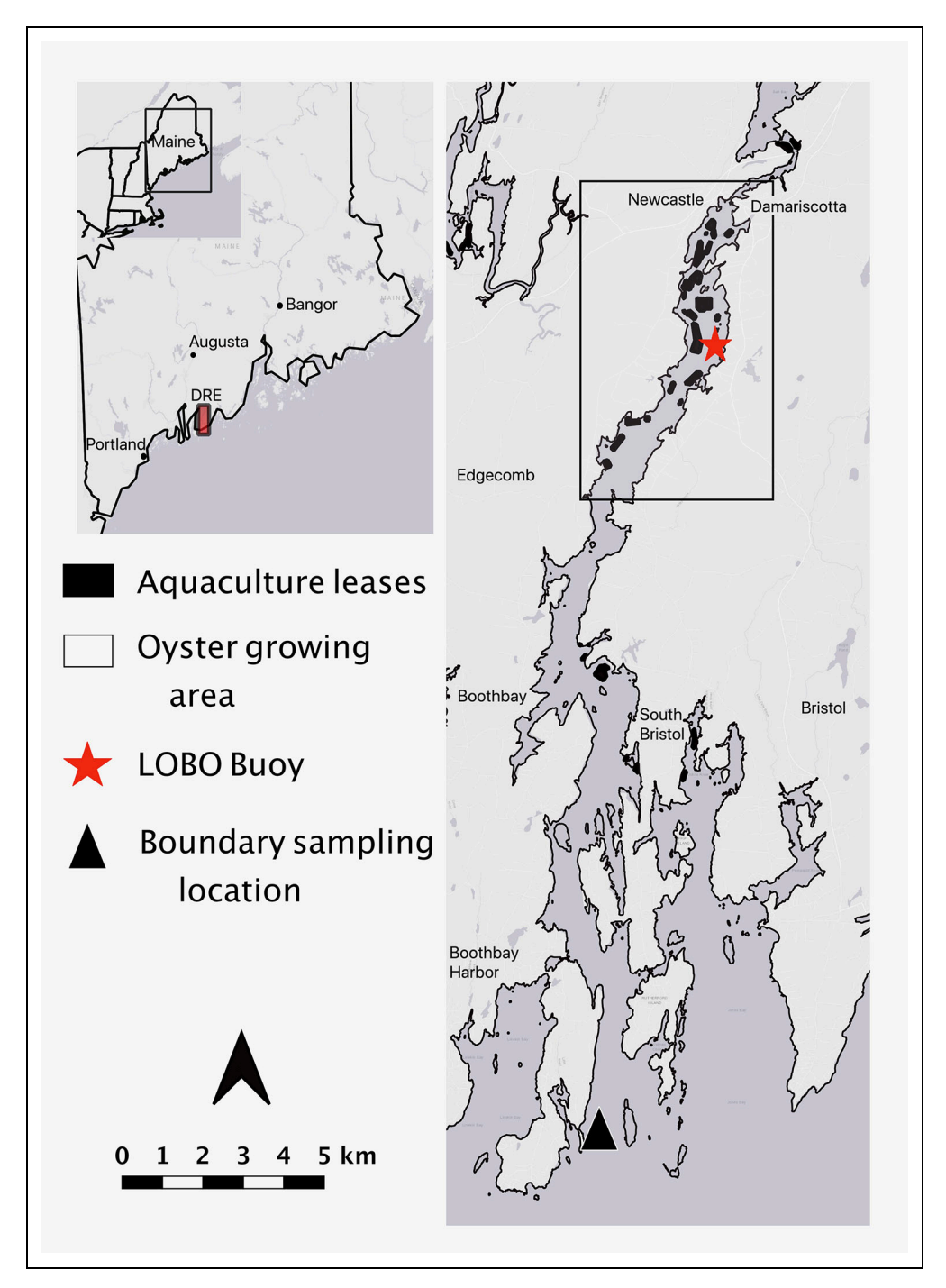


Figure 2. The Damariscotta River Estuary in Maine. The black box in the right-hand map represents the area treated as the growing area zone in the model. The Land-Ocean Biogeochemical Observatory (LOBO) buoy was deployed in the middle of the growing area for the entire growing season of 2018. TA, DIC, temperature, and practical salinity were measured at the LOBO buoy and mouth of the river where it meets the open Gulf of Maine. DOI: https://doi.org/10.1525/elementa.2020.00057.f2

represents the principal source of water for the ocean-dominated Damariscotta River Estuary because the largest freshwater source only contributes 1–3 m³ s⁻¹ on average during the growing season (McAlice, 1977; and unpublished data from Damariscotta Mills Dam, Kruger Energy, 2015–2018; **Figure 2**). A Land-Ocean Biogeochemical Observatory buoy (LOBO; Jannasch et al., 2008), positioned within the growing area, collected hourly temperature, practical salinity, and dissolved oxygen data

throughout the season. Additionally, we measured physiochemical properties (TA, DIC, practical salinity, and temperature at 1-m depth) of the growing area and Gulf of Maine source water by sampling at the LOBO buoy and mouth of the Damariscotta River Estuary where it meets the Gulf of Maine, respectively (**Figure 2**), monthly to biweekly from June to September 2018 (6 samplings total). A profile of the whole water column in both locations measured temperature, practical salinity, dissolved

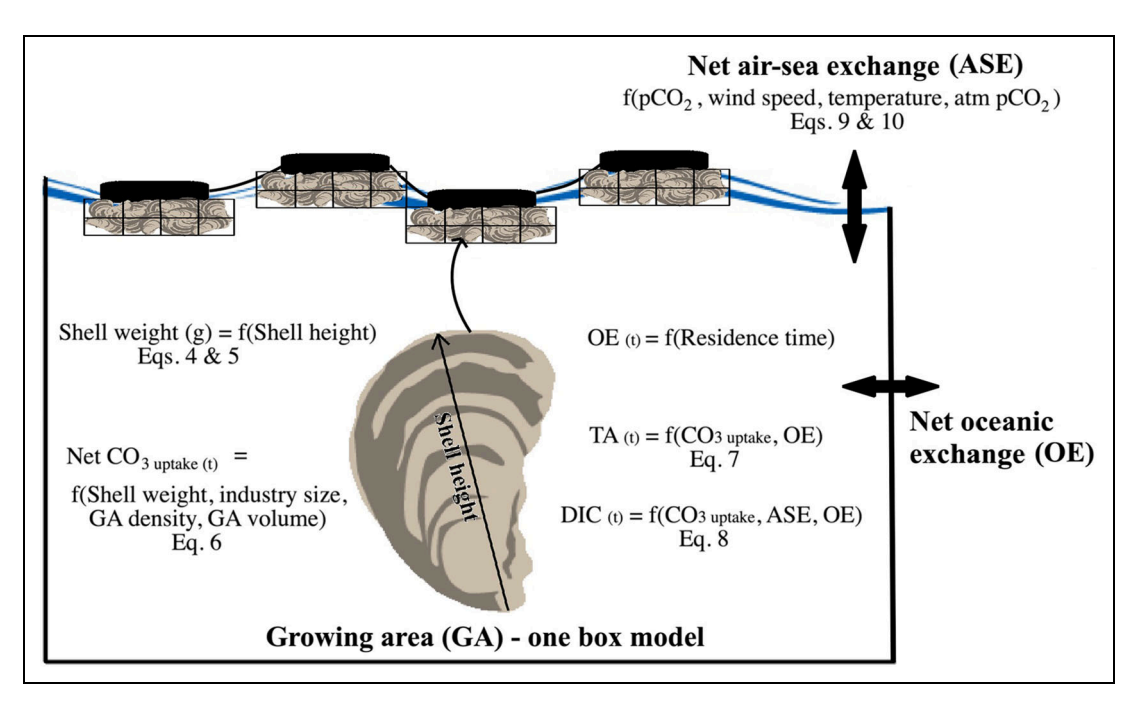


Figure 3. Conceptual diagram of the model. Distributions of shell heights and their growth were converted to net calcification rates and then to net changes in TA and DIC due to net calcification and gross respiration. These changes were scaled to various industry sizes assuming constant shell size distributions. CO_2 exchange with the atmosphere was calculated based on computed pCO_2 in water and assumed values in air. Water in the growing area was exchanged with the oceanic endmember (OE) at rates parameterized by residence time calculations from our hydrodynamic model. DOI: https://doi.org/10.1525/elementa.2020.00057.f3

oxygen, pH, and chlorophyll a during each sampling; it confirmed that the estuary was well-mixed tidally throughout the year.

Sample collection and analysis

Salinity, temperature, pH, DO, and chlorophyll *a* were measured using a YSI 6920 multiparameter sonde that was calibrated the day prior to sampling using YSI solutions or recommended calibration practices. Triplicate TA and DIC samples were collected using a Niskin sampler from 1-m depth and transferred to 60-ml borosilicate glass bottles using clean flexible tubing. The tube was placed at the bottom of the bottle and the bottle was inverted to allow water to coat all sides to avoid forming bubbles. The bottle was then turned upright, and water was allowed to overflow the bottle for 10 s, or approximately 250 ml. Less than 1% headspace was left in the bottles, which were kept on ice until return to the laboratory refrigerator before analysis. Samples were analyzed within 24 h of collection.

TA was analyzed using potentiometric titration in an open cell titration, following the methods described in Guide to Best Practices for Ocean CO₂ (Dickson et al., 2007). Briefly, samples were kept in a water bath at 25°C for 10 min prior to analysis, and a weighed sample was then placed in a jacketed beaker maintained at 25°C. A calibrated liquid junction pH electrode was submerged in the sample with a magnetic stir bar that gently mixed the sample continuously; 0.1N hydrochloric acid was added to the sample at a rate slower than 0.05 ml s⁻¹ until the pH reached 2.9. The titration data were then used with the package SeaCarb in R (Gattuso et al.,

2020) to calculate the TA of the system. The average standard deviation across all triplicate samples for TA was \pm 9.7 µmol kg⁻¹. DIC was analyzed using a Shimadzu TOC-4200 analyzer. A known volume of room temperature seawater was drawn into a chamber where it was acidified with 8.5% phosphoric acid solution and the off-gassed CO₂ was extracted using a pure nitrogen gas stream. CO₂ was then measured using a nondispersive infrared radiation detector. The full methods can be found in O'Sullivan and Millero (1998). The average standard deviation across all triplicate samples for DIC was \pm 6.0 µmol kg⁻¹. Certified reference materials from the A Dickson Lab at Scripps Institution of Oceanography were used to standardize both TA and DIC samples.

Oyster aquaculture in the growing area and organismal activity

All oyster aquaculture in Maine occurs in subtidal waters. In the growing area, some companies start the oysters in surface rafts and then spread animals onto the bottom for the second year of growth, while the majority of companies use surface culture for both years until harvest (C Davis of Pemaquid Oyster Co, personal communication, June 6, 2019). The oyster growing season is generally when the water temperature is above 10°C, most often spanning early May to late October. The growth of oysters over both first and second growing seasons was estimated as the average change in shell height over the season (**Figure 3**) with input from industry partners (C Davis of Pemaquid Oyster Co and M White of Mook Sea Farm, personal communication, October 13, 2020). These two

Table 1. Model inputs for both simulation years 2018 and 2050. DOI: https://doi.org/10.1525/ elementa.2020.00057.t1

Year	TA (μmol kg ⁻¹)	DIC (μmol kg ⁻¹)	Practical Salinity	Temperature (°C)	Shell Weights (g CaCO ₃)	Wind Speed $(m s^{-1})$	Atmospheric <i>p</i> CO ₂ (ppm)
2018	2091	1926	31.36	10.6–24.14	0.38-48.36	0-2.25	409
2050	2091	1966	31.36	11.1-24.64	0.38-48.36	0-2.25	550

DIC = dissolved inorganic carbon; TA = total alkalinity.

companies have been farming in the growing area for over 30 years and provided an interannual average change in oyster shell height for both first- and second-year oysters that they grow. The two estimates were averaged to produce the change in shell height by year used in the model. Calcium carbonate uptake (i.e., shell deposition—dissolution) was estimated by applying shell height to shell dry weight relationships developed in the growing area (Fig**ure 3**). We measured seed oyster shell height (2–20 mm) and dry shell weight in 2017, and Adams et al. (2019) measured oyster shell height (40-100 mm) and dry shell weight in 2017. Here, shell height is defined as the distance between the bottom-most section of the hinge to the middle of the top edge (**Figure 3**).

We estimated the dry shell weight of oysters between 2 and 20 mm using the equation derived from our growth study:

Shell weight (g) =
$$0.0123 *$$
 Shell height (mm) + 0.2958 . (4)

We estimated dry shell weight of oysters between 21 and 90 mm using the shell heights and dry weights measured by Adams et al. (2019):

Shell weight (g) =
$$0.0069 *$$
 Shell height (mm)
- $0.1586 *$ Shell height (mm) + 1.1567 .

We assumed dry shell weight was 100% CaCO₃ and that other components of shell (e.g., protein matrix, periostracum) were negligible (Marie et al., 2011). Because these oysters are harvested and then largely exported to other watersheds, this net growth represents net calcification within the growing area.

Harvest throughout the growing season removes second-year oysters as they reach different size classes, reducing the total number of oysters left in the system to calcify and respire. To incorporate the impact of harvest on carbonate removal, we assumed that 25% of oysters are harvested at "cocktail" size (65-75 mm), 50% of oysters are removed at "select" size (75-85 mm), and the remaining 25% are harvested as "jumbo" oysters (>85 mm; C Davis of Pemaquid Oyster Co, personal communication, October 8, 2020).

Model strategy

We developed a one box model (Figure 3) of the impact of oyster net calcification and gross respiration on carbonate chemistry change using Damariscotta River Estuary input values of oyster shell height, temperature, practical salinity,

TA, DIC, atmospheric pCO₂, and wind (**Table 1**). We used the seasonally averaged values of TA, DIC, and practical salinity measured at the mouth of the estuary (Figure 2) as the initial and ocean boundary water chemistry conditions for the model. The freshwater contribution to the estuary was not included due to its extremely low input during the growing season. We therefore kept salinity constant throughout the model runs to avoid errors that would arise from using TA and DIC measured at the mouth of the river with slightly higher salinity than in the growing area. Daily averaged temperature data from the LOBO buoy were used to capture seasonal changes in radiative heating and cooling.

Model variables included TA, DIC, industry size, water residence time in the growing area, in situ pCO_2 , Ω_{CA} , and Ω_{AR} (**Table 2**). In situ pCO_2 was used to calculate air-sea exchange and adjust remaining DIC concentrations. The model used a daily time step and estimated daily growth rates for oysters in the upper Damariscotta River Estuary to calculate changes in TA and DIC while accounting for air-sea and oceanic exchanges. We focused the model on the potential impact from oyster growth on carbonate chemistry. We did not include other processes affecting the carbonate system, such as primary production, benthic processes, dissolution, and nutrient dynamics, but their potential contributions are discussed.

For each mole of CO_3^{2-} removed for calcification, the model removed 2 moles of TA and 1 mole of DIC. Lejart et al. (2012) found that molar CO2 production from respiration was 3 times higher than the net molar calcium carbonate uptake for adult Pacific oysters, Crassostrea gigas. Assuming this ratio for Crassostrea virginica, water column DIC was increased by 3 moles from respiration for each mole of CaCO₃ derived from shell growth. To scale these estimates to commercial aquaculture scenarios, we modeled between 0 and 50 million oysters in the system to represent a spectrum of no aquaculture to a potential future industry size in the growing area (Table 2). When oysters were present, they were modeled as continuously submerged (i.e., no desiccation regime) for their entire life span in the system. The 2018 industry size was estimated as 16 million oysters by assuming that the 2018 oyster landings from the Damariscotta River (approximately 8 million oysters; Maine Department of Marine Resources, 2020) represent half of cultured oysters in the growing area, given 2 years of growing time required for seed to reach market size (C Davis of Pemaquid Oyster Co, personal communication, January 24, 2018). A potential industry size of 50 million oysters was chosen for the year 2050 by extrapolating the current growth rate

Table 2. Model variables used in both 2018 and 2050 simulations. DOI: https://doi.org/10.1525/elementa.2020.00057.t2

TA (μmol kg ⁻¹)	DIC (μmol kg ⁻¹)	Industry Size (millions)	Residence Time (days)	In Situ <i>p</i> CO ₂ (ppm)	Ω
Calculated daily from oyster growth and oceanic exchange	Calculated daily from oyster growth, oceanic exchange, and air-sea exchange	0–50	6–20	Calculated daily from TA, DIC, temperature, and salinity	Calculated daily from TA, DIC, temperature, and salinity

DIC = Dissolved inorganic carbon; TA = total alkalinity.

(approximately 1 million more oysters in the growing area each year) to the year 2050. Although other factors such as physical space, food supply, and competing uses may limit this growth (Johnson et al., 2019), we modeled this possible industry size to aid our exploration of the history of aquaculture in this system, as well as market and policy implications for shellfish aquaculture development in the Gulf of Maine (The Hale Group, Ltd and Gulf of Maine Research Institute, 2016).

We used the model to isolate the impact of individual processes by modeling the changes in Ω resulting from alterations of one process at a time. For example, oyster net calcification effects on TA, DIC, and Ω were modeled by excluding respiration and oceanic exchange and holding temperature and salinity constant.

To explore the role that OCA may have in changing Ω and the interaction with oyster growth, we examined the combined effects of net calcification and gross respiration on Ω_{CA} with changes in temperature and DIC due anthropogenic increases in CO₂ projected for the year 2050, using the "business as usual," RCP 8.5 emissions scenario (IPCC, 2014). Gulf of Maine DIC is predicted to increase an average of 1.25 µmol kg⁻¹ yr⁻¹ from increasing atmospheric CO₂ (Siedlecki et al., 2021). Siedlecki et al. (2021) utilized a coupled physical-biogeochemical model developed by Gehlen et al. (2015) and a physical model (Regional Ocean Modeling System; Shchepetkin and McWilliams, 2005) paired with an empirical model developed by McGarry et al. (2021) to estimate changes in DIC, TA, and Ω in the Gulf of Maine in 2050 using RCP 8.5. We therefore adjusted the initial DIC concentration from the current concentration of 1926 μmol kg⁻¹ to the predicted value of 1966 μmol kg⁻¹. We also increased the atmospheric pCO₂ to 550 ppm in accordance with estimates from RCP 8.5 (IPCC, 2014). The temperature of the Gulf of Maine has been increasing rapidly this century (Friedland et al., 2020a; Friedland et al., 2020b; Goncalves Neto et al., 2021) and is expected to continue warming. Brickman et al. (2021) also used the same downscaled global models as Siedlecki et al. (2021) to estimate that the Gulf of Maine will warm by an additional 0.5°C by 2050 compared to average 2018 temperatures using the RCP 8.5 emissions scenario. Thus, we added 0.5°C to the daily 2018 temperatures for the 2050 model scenarios.

We estimated the 2018 residence time for the growing area using a realistic 3-dimensional hydrodynamic model we developed for the mid-coast of Maine, including the

Damariscotta River Estuary (see Text S1 for full description). We modeled a range of residence times (i.e., oceanic exchange; **Figure 3**, **Table 2**) from 6 to 20 days to explore model sensitivity and reflect that how residence time is calculated (e.g., freshwater replacement time, tidal prism method, isohaline decomposition analysis) can affect our understanding of how Ω varies. Additionally, climate change is predicted to reduce estuarine residence times through increased precipitation and therefore flushing (Scavia et al., 2002) and increased sea level rise and tidal changes (Du et al., 2018). The model was run for each combination of residence time and industry size (**Table 2**). The CO2SYS program (van Heuven et al., 2011) was used to estimate the daily Ω using the variable temperature, TA, DIC, and average seasonal salinity. We used the K₁ and K₂ dissociation constants derived by Mehrbach et al. (1973) and refit by Dickson and Millero (1987), the KSO₄₋ disassociation constants by Dickson et al. (1990), and total borate constant of Uppström (1974). Thus, the model uses 3 key inputs to estimate the impact of oyster growth and physical processes on Ω (**Figure 4**): (1) oyster shell daily weight gain (g CaCO₃ day⁻¹) of both first- and second-year oysters combined, (2) daily average water temperature (°C), and (3) wind speed (m s⁻¹) measured at the nearby Wiscasset Airport (Menne et al., 2019).

Finally, we modeled a scenario where we excluded the impact of oyster respiration on Ω . This scenario assumes the CO_2 produced through respiration was utilized for photosynthesis within the growing area or removed through another avenue not modeled here rather than directly released into the water column. All other model forcing functions (i.e., air-sea and oceanic exchange formulations, and seasonal temperature) and scenarios (i.e., industry sizes, residence times, and climate conditions) were as described above.

Several assumptions were necessary to simplify model setup and analysis. First, we omitted any freshwater entering the growing area because the largest freshwater source only contributes 1–3 m³ s⁻¹ on average to the growing area. Variable salinity should be included for other systems where freshwater is a larger contributor. Second, we omitted changes in TA due to ammonia excretion by oysters. Data from this estuary has shown that there has not been an increase in the standing stock of ammonia over the last 25 years (Mayer et al., 1996, and unpublished data from K Thornton, University of Maine, 2017–2019) despite a more than 10-fold increase in the number of oysters in the

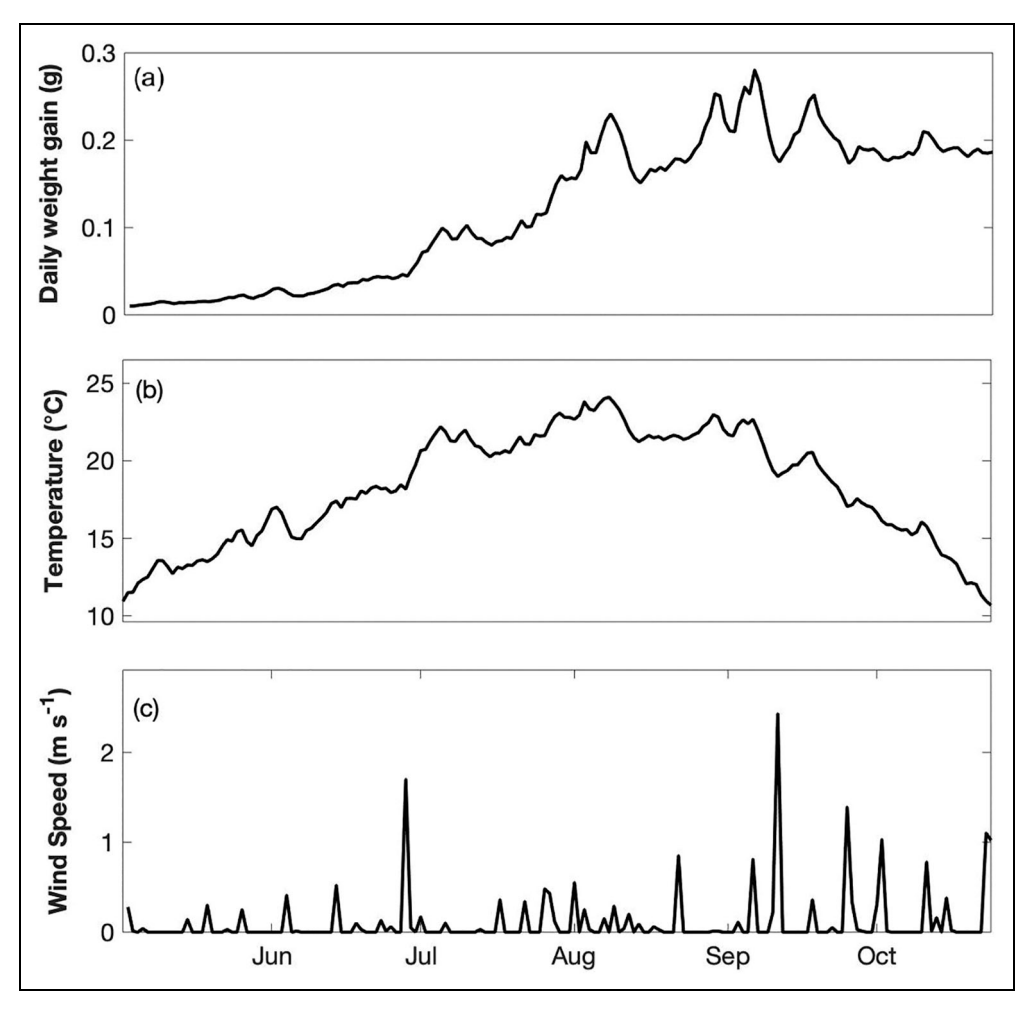


Figure 4. Model inputs of oyster shell height, temperature, and wind speed over the growing season. (a) Estimated average daily oyster weight gain (g CaCO₃) for both first- and second-year oysters, (b) daily average temperature (°C), and (c) daily averaged wind speed (m s⁻¹). DOI: https://doi.org/10.1525/elementa.2020.00057.f4

system (Maine Department of Marine Resources, 2020). Although excretion of ammonia by oysters may lead to an increase in TA (Lejart et al., 2012) on short time scales (hours to days), the ammonia is removed from the system quickly either through primary production or oxidation to yield an assumed net-zero effect on TA. Third, dissolution of dead shells can also be a source of TA to an estuary from natural oyster reefs (Waldbusser et al., 2013; Shen et al., 2019). However, we did not incorporate dissolution because we based our industry sizes on harvest data; thus, all modeled oysters were removed from the system through harvest and exported and did not remain in the growing area where their dissolution could affect Ω . No shells are returned to the estuary after harvest per state law. Loss of oysters (i.e., settling to the bottom to remain in the estuary) during grow-out and harvest is thought to be very low but might provide neutralization of acidification over the decades; however, we have no data to include this process quantitatively in a model of this type. Dissolution should be included in models of systems with natural oyster reefs, when dead shells are returned to the water body, or calculations in aquaculture systems where the amount of product loss is known or well estimated.

Finally, oysters can use a fraction of the CO₂ produced through respiration as the carbon source for calcification rather than simply releasing the CO₂ to the water column. Previous studies have shown that, on average, 10% of bivalve shell mass is derived from respired CO2 (McConnaughey et al., 1997; Lorrain et al., 2004; Gillikin et al., 2006), although Gillikin et al. (2007) found a significantly higher fraction (5%-37%) in hard clams (Mercenaria mercenaria) from North Carolina. Given the uncertainties in the amount of respired carbon used for calcification in eastern oysters, and the estimated small fraction used by other bivalves, we did not incorporate the impact from metabolic carbon usage on DIC, but we see value in improving this model in the future by incorporating a more detailed carbon tracking process for oysters as requisite details become available.

Model equations

The CO_3^{2-} removed per oyster was calculated using the average shell weight gain each day, converted from grams to micromoles. We used the following equation to estimate total CO_3^{2-} uptake:

$$CO_{3 \text{ uptake}} = \frac{\text{shell}_{wg} * \text{industry size}}{\text{density}_{GA} * \text{volume}_{GA}},$$
 (6)

where $CO_{3uptake}$ is the amount of CO_{3}^{2-} removed from the water for shell growth (µmol kg⁻¹ day⁻¹), shell_{wg} is the amount of shell gained each day by both year-1 and year-2 oysters averaged together (µmol $CaCO_{3}$ day⁻¹ oyster⁻¹), estimated using Equations 4 and 5. Density_{GA} is the average water density in the growing area calculated from temperature and salinity (kg-water l-water⁻¹; Moataz, 2021), volume_{GA} is the average volume of the growing area (l-water; McAlice, 1977), and industry size is the number of oysters in the growing area each day for both first-and second-year oysters.

We calculated TA each day using:

$$TA_{(t)} = (1 - F) * \left(TA_{(t-1)} - 2 * \left(CO_{3 \text{ uptake }(t)}\right)_{calc}\right) + F * TA_{OE},$$
 (7)

where $TA_{(t)}$ is the total alkalinity after net calcification, F is the fraction of water replaced each day in the growing area due to tidal exchange (F = t/Residence Time), $TA_{(t-1)}$ is the TA from the previous day, CO_3 uptake calc is the amount of CO_3^{2-} removed from the growing area each day by oyster calcification, and TA_{OE} is the average TA at the mouth of the Damariscotta River Estuary, held constant at 2091 μ mol kg⁻¹. All concentrations are in μ mol C kg⁻¹.

DIC was calculated similarly to TA but with the addition of oyster respiration and air-sea exchange. DIC was reduced by 1 mole for each mole of calcification and was increased by 3 moles from respiration for each mole of net calcification. Therefore,

$$DIC_{(t)} = (1 - F) * (DIC_{(t-1)} - (CO_{3 \text{ uptake}(t)})_{\text{calc}}$$

$$+ 3 * (CO_{3 \text{ uptake}(t)})_{\text{resp}} - (DIC_{(t)})_{\text{ASE}})$$

$$+ F * DIC_{\text{OE}},$$
(8)

where $DIC_{(t)}$ is the concentration of DIC at the end of the day after all processes are included, F is the fraction of water replaced each day due to oceanic exchange, $DIC_{(t-1)}$ is the DIC concentration from the previous day, $CO_{3\text{ uptake calc}}$ is the daily loss of DIC from net calcification, $CO_{3\text{ uptake resp}}$ is the daily addition of DIC from oyster respiration, DIC_{ASE} is the daily amount of DIC exchanged with the atmosphere due to gas transfer, and DIC_{OE} is the average DIC at the mouth of the Damariscotta River Estuary (1926 μ mol kg $^{-1}$). All variables are in μ mol C kg $^{-1}$.

Air-sea exchange

We used TA and DIC calculated from daily oyster shell growth and respiration to calculate the partial pressure of carbon dioxide (pCO_2) in the water using the program CO2SYS (van Heuven et al., 2011) and the same constants as above. We used the "tracers only" gas transfer velocity (k_{600}) equation (Raymond and Cole, 2001) and converted to a saltwater formulation (k_{660}) using the calculated Schmidt number and coefficients from Wanninkhof (2014). We chose the Raymond and Cole (2001) gas transfer velocity equation because it was formulated for

estuaries with wind speeds between 0 and 7 m s⁻¹ which are typical in the growing area. The gas transfer velocity was calculated as:

$$k_{660} = 1.58e^{0.30x} * (Sc/660)^{-0.5},$$
 (9)

where x is the wind speed (m s⁻¹) measured at 10 m above the ground and Sc is the Schmidt number calculated each day. The air-sea flux was calculated using:

$$CO_{2 \text{ flux}} = k_{660} * CO_{2 \text{ sol}} * (pCO_{2 \text{ w}} - pCO_{2 \text{ atm}}),$$
 (10)

where CO_2 sol is the solubility of CO_2 calculated from temperature, salinity, and pressure, pCO_2 w is the calculated in situ pCO_2 , and pCO_2 atm is the atmospheric CO_2 concentration.

Using the calculated partial pressure of carbon dioxide in the water, water temperature, practical salinity, wind, and an average atmospheric pCO_2 concentration (409 and 550 ppm for 2018 and 2050, respectively), we estimated the amount of CO_2 that transfers to or from the atmosphere each day and adjusted the DIC pool to reflect this flux. The 2018 atmospheric pCO_2 concentration was measured on a buoy in the western Gulf of Maine (NOAA Pacific Marine Environmental Lab/University of New Hampshire Coastal CO_2 Buoy D).

Results

First-year oysters were estimated to grow from 2 to 45 mm and second-year oysters from 46 to 90 mm between early May and late October. Daily oyster shell weight gain assuming equal numbers of first- and second-year oysters combined was 0.0101 g CaCO₃ oyster⁻¹ day⁻¹ in the beginning of May, and increased to a maximum of 0.25 g CaCO₃ oyster⁻¹ day⁻¹ in early September (**Figure 4a**). Temperature varied on a seasonal cycle, beginning at 10.9°C in early May, peaking at 24°C in early August, and ending at 10.6°C in late October (Figure 4b). Daily average wind speed was low (0-2 m s⁻¹) but representative of the relatively protected upper estuary (Figure 4c). The measured DIC and TA concentrations in the center of the growing area for the beginning, middle, and end of the season were 1963, 1960, and 1798 μmol kg⁻¹, respectively, for DIC and 2166, 2084, and 2129 μmol kg⁻¹, respectively, for TA. These measured values were corrected to a salinity of 31.36 to match the model salinity, but they incorporate impacts from other estuarine processes not modeled here. The modeled DIC and TA for the beginning, middle, and end of the season in the growing area were 1933, 1885, and 1929 μmol kg⁻¹, respectively, for DIC and 2091, 2080, and 2080 μmol kg⁻¹, respectively, for TA.

The modeled DIC decreased from 1929 μ mol kg⁻¹ to 1888 μ mol kg⁻¹ in the first half of the growing season regardless of oyster presence (**Figure 5a**), largely due to degassing driven by increased temperature. During the second half of the growing season, the modeled DIC with both 0 and 16 million oysters increased toward the initial concentrations, reaching 1939 and 1933 μ mol kg⁻¹, respectively, by the end of October. Between mid-August and the end of October, 16 million oysters lowered the DIC by 3.4 μ mol kg⁻¹ on average (**Figure 5a**). The TA remains

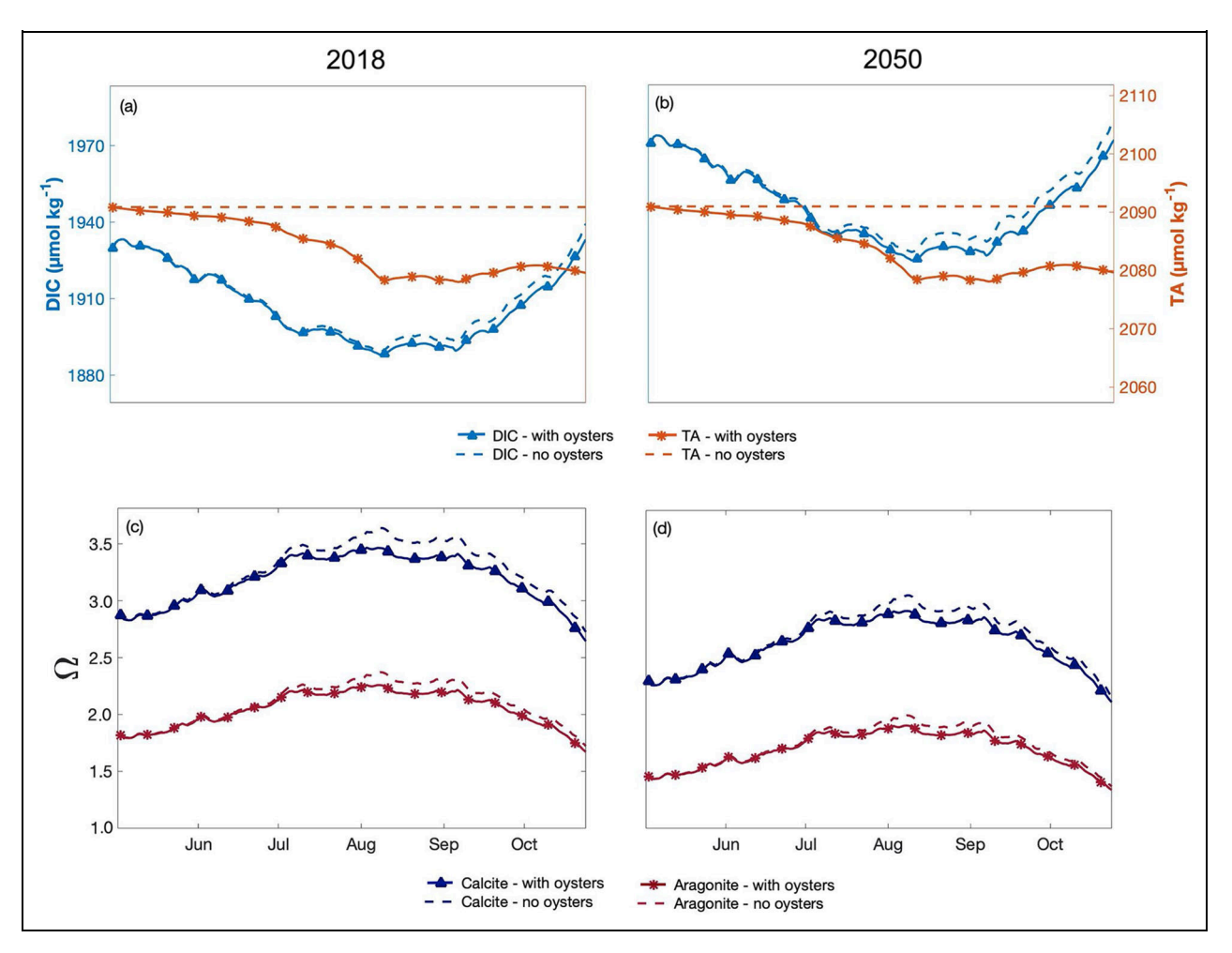


Figure 5. DIC, TA, Ω_{CA} , and Ω_{AR} modeled with 2018 and 2050 oceanic conditions. (a, b) DIC and TA, (c, d) Ω_{CA} and Ω_{AR} in the growing area modeled with the (a, c) 2018 and (b, d) 2050 oceanic conditions. An industry size of 16 million oysters (solid lines) and zero oysters (dashed lines) were modeled for both oceanic conditions, all with a residence time of 13 days. DOI: https://doi.org/10.1525/elementa.2020.00057.f5

constant throughout the zero oyster scenario because oyster growth is the only process removing TA in the model. In the 16 million oyster scenario, the TA decreases slowly between early May and mid-June (<5 μmol kg⁻¹ lost by mid-June), and then decreases more rapidly until early August when it levels off at 2080 μmol kg⁻¹ for the rest of the season (Figure 5a). The Ω_{CA} increased by 0.6 units between early May and early August reaching a maximum of 3.63 in the zero oyster scenario, whereas the Ω_{AR} increased by 0.5 units during the same time period, with a maximum of 2.37. The inclusion of oysters lowered Ω_{CA} and Ω_{AR} by 0.11 and 0.07 units, respectively, on average between July and the end of October, with a maximum difference of 0.18 and 0.11 units, respectively, in early August. While the trends in DIC, TA, and Ω remained the same for the 2050 OCA model, the average DIC for the growing season increased and Ω decreased (**Figure 5c** and d). The maximum change in DIC over the season increased from 45.1 µmol kg⁻¹ in 2018 to 48.9 µmol kg⁻¹ in 2050. The TA was not altered by the 2050 conditions. The average Ω_{CA} and Ω_{AR} for the growing season decreased by 0.55 and 0.35 units, respectively. However, the maximum

change in both Ω_{CA} and Ω_{AR} over the growing season did not vary between 2018 and 2050.

The net changes in these carbonate parameters result from accumulated impacts of daily biological and physical processes. Oyster respiration and net calcification had minimal impact (<0.05 μmol kg⁻¹ day⁻¹) on DIC during slow oyster growth before July, but these impacts increased throughout the season, with respiration increasing Δ DIC twice as much as calcification decreased it (2 and 1 μmol kg⁻¹ day⁻¹, respectively; **Figure 6a**). Air-sea exchange of CO₂ due to oyster growth reduced ΔDIC by a similar magnitude as oyster respiration increased it, relative to the initial conditions. However, the air-sea exchange of CO₂ lagged behind production via respiration by 1 week (Figure 6a). Oceanic exchange raised DIC by 1.6 μmol kg⁻¹ day⁻¹ on average, mirroring losses from airsea exchange. TA was altered by two counterbalancing processes, net calcification and oceanic exchange. Net calcification was slow before July with minimal impact on TA (<0.33 μmol kg⁻¹ day⁻¹). However, between July and late October, TA decreased by 0.90 µmol kg⁻¹ day⁻¹ on average. Oceanic exchange increased TA by 0.82 µmol kg⁻¹ day⁻¹

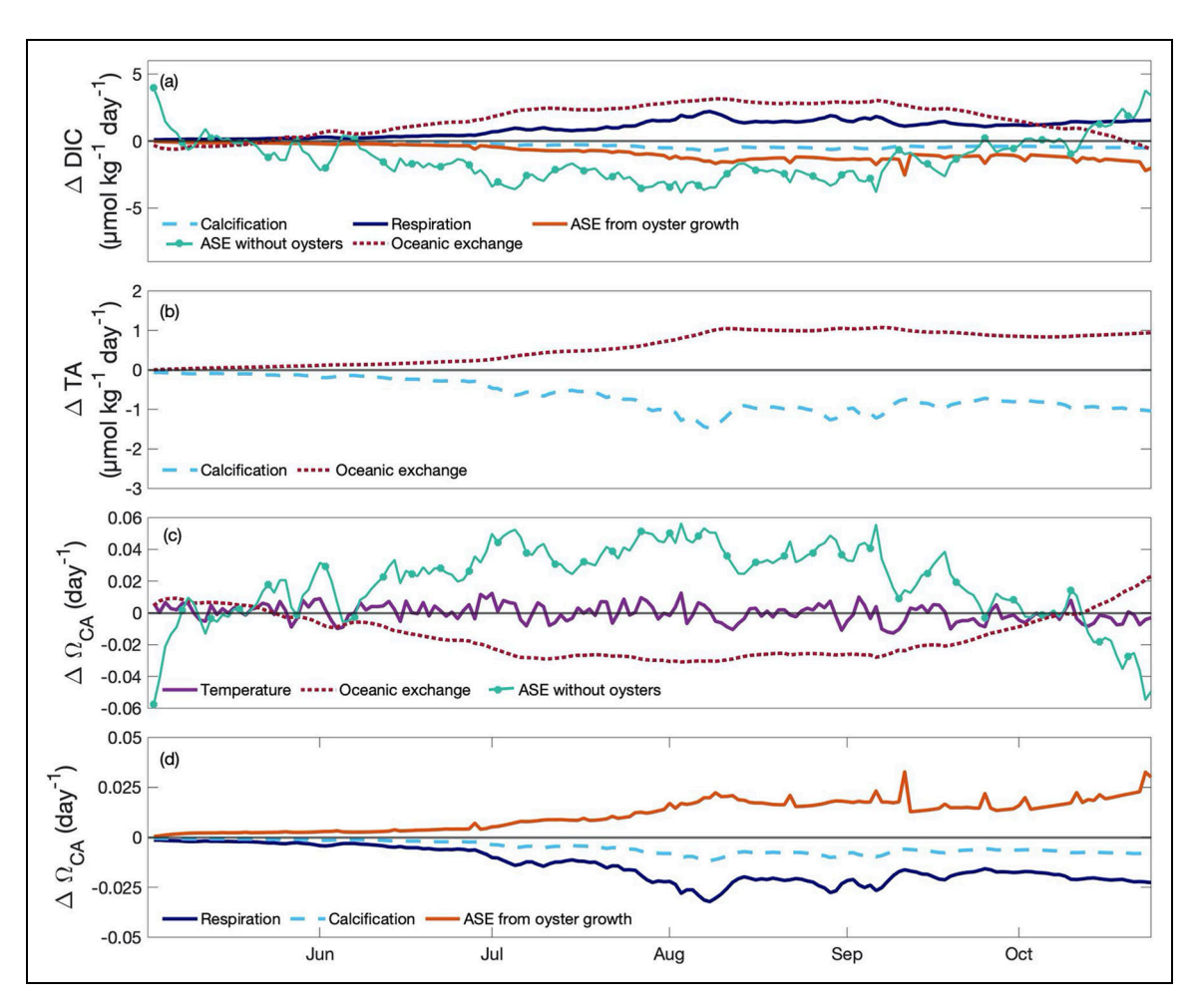


Figure 6. Individual process contributions to changes in DIC, TA, and Ω_{CA} . Daily changes in (a) DIC, (b) TA, and (c, d) Ω_{CA} in the growing area to a water mass assumed to have conditions equal to the incoming ocean end member, broken out as contributions from calcification, respiration, ambient air-sea exchange, air-sea exchange due to oyster growth, oceanic exchange, and temperature change. Panel (c) shows changes in Ω_{CA} from physical processes and panel (d) shows changes in Ω_{CA} from biologically driven processes. Calculations are for conditions of 13-day residence time and 16 million oysters. DOI: https://doi.org/10.1525/elementa.2020.00057.f6

on average, which restored TA back toward the boundary conditions at the current industry size (**Figure 6b**).

The daily temperature impact on Ω_{CA} was net positive (0.0017 units day⁻¹ on average) over the first half of the season, and net negative (-0.0017 units day⁻¹ on average) over the second half of the season (Figure 6c), mirroring the seasonal change in temperature. Non-oyster driven airsea exchange initially decreased Ω_{CA} by up to 0.06 units day⁻¹ as the water was undersaturated in the beginning of May and absorbs CO₂ from the atmosphere. However, after mid-May, air-sea exchange increased Ω_{CA} by up to 0.04 units day⁻¹ until late October when air-sea exchange lowered Ω_{CA} by up to 0.06 units day⁻¹ again. The air-sea exchange pattern is driven mostly by seasonal temperature changes (Figure 6c). Oceanic exchange counterbalanced change in Ω_{CA} from oyster growth and air-sea exchange throughout the season; $\Delta\Omega_{CA}$ values of up to -0.03 units day⁻¹ from oceanic exchange occurred in August when DIC was being lost to the atmosphere at a higher rate than TA and DIC were being lost due to calcification. Net oyster calcification and gross respiration have minimal impact prior to July but decreased Ω_{CA} in

the latter half of the season by up to 0.01 and 0.026 units day $^{-1}$, respectively (**Figure 6d**). Air-sea exchange due to oyster growth was negligible for the first part of the growing season but became more substantial (increasing Ω_{CA} by 0.025 units day $^{-1}$) toward the end of the growing season.

Increasing industry size and 2050 climate conditions (assuming a RCP 8.5 scenario) both significantly lowered Ω , particularly during the latter half of the growing season (**Figure 7a** and **b**). Modeling Ω using only the physical processes (zero oysters) and the 2050 climate conditions decreased Ω_{CA} and Ω_{AR} by 0.57 and 0.37 units, respectively, on average over the growing season compared to the 2018 climate conditions with zero oysters. Increasing the industry size to 50 million oysters caused net calcification and gross respiration to decrease Ω_{CA} and Ω_{AR} by 0.16 and 0.10 units on average under 2018 climate conditions. Alternatively, keeping the industry size constant at 16 million oysters, but under modeled 2050 carbonate chemistry conditions, lowered Ω_{CA} and Ω_{AR} by an average of 0.55 and 0.35 units, respectively, over the growing season with a maximum reduction of 0.57 and 0.36 units,

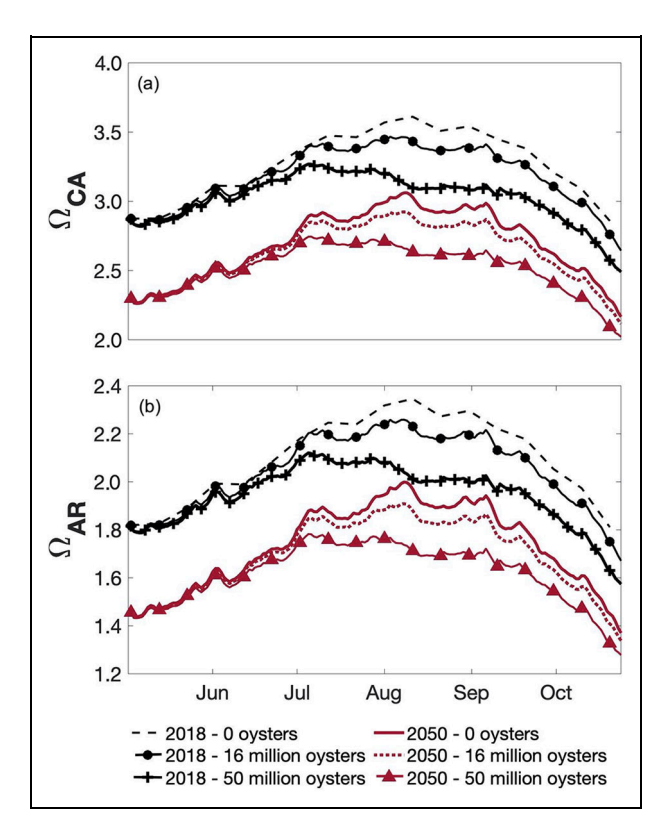


Figure 7. Impact of oyster growth on Ω under 2018 and 2050 carbonate chemistry conditions. (a) Ω_{CA} and (b) Ω_{AR} were calculated with a 13-day residence time, with 0,16, and 50 million oysters, and with both 2018 climate conditions (black) and forecast 2050 climate conditions (red) (increased water temperature, DIC, and atmospheric pCO_2). DOI: https://doi.org/10.1525/elementa.2020.00057.f7

respectively, in early August. The combination of 2050 carbonate chemistry conditions and 50 million oysters lowered Ω_{CA} and Ω_{AR} by 0.67 and 0.43 units, respectively, on average for the latter half of the growing season when compared to 2018 climate conditions and industry size.

Variation in water residence time had a smaller effect on Ω than increasing industry size and 2050 climate conditions. In the first third of the growing season under 2018 conditions, residence time had almost no effect on Ω , but from July to September, decreased residence time resulted in lower Ω . Then, for the month of October, decreased residence time increased Ω (**Figure 8a**). Residence time had minimal impact on Ω when the industry size increased to 50 million oysters and modeled with 2018 climate conditions, with lower residence time slightly lowering or raising Ω at different times in the season (Figure 8b). With 2018 industry size and 2050 climate conditions, shorter residence time led to decreased Ω throughout the season (**Figure 8c**). The model combination of 2050 climate conditions and 50 million oysters was similar to the 2050 scenario with the 2018 industry size (Figure 8d).

Oyster growth affects Ω through net calcification and respiration and was sensitive to industry size and OCA conditions (**Figure 9**). In 2018 scenarios (**Figure 9**a

and **c**), oyster growth lowered Ω relative to the zero oyster scenario regardless of how many oysters were included in the simulation. Calcification of 16 million oysters lowered Ω_{CA} and Ω_{AR} by 0.03 and 0.02 units, respectively, on average, whereas calcification and respiration combined lowered Ω_{CA} and Ω_{AR} by 0.08 and 0.05 units, respectively, on average over the growing season. Calcification of 50 million oysters reduced Ω by nearly the same magnitude as calcification and respiration of 16 million oysters. The same trends were observed for scenarios modeled with 2050 climate conditions, but the relative difference between impacts of the various scenarios decreased as overall Ω decreased (**Figure 9b** and **d**).

Discussion

Ocean acidification research has consistently shown that most calcifying organisms will likely be negatively impacted by anthropogenic alterations in carbonate chemistry (Miller et al., 2009; Gazeau et al., 2013; Waldbusser and Salisbury, 2014; Gledhill et al., 2015; Waldbusser et al., 2015; Ekstrom et al., 2015). However, studies rarely consider aquaculture settings where calcifying organisms can enhance acidification of their own surroundings (Mistri and Munari, 2012; Munari et al., 2013; Morris and Humphreys, 2019; Li et al., 2021), with implications for the sustainable carrying capacity. This modeling study shows how these organisms potentially influence estuarine carbonate chemistry in addition to the atmospherically mediated changes. This quantitative framework highlighted that the counterbalancing effects of air-sea exchange and higher temperatures on Ω will make measuring the impact on Ω by oysters in situ difficult. Furthermore, there will be unpredictable interactive impacts of other processes that affect Ω , such as photosynthesis and respiration of other organisms, nutrient fluxes in the water column or from the sediments, and large precipitation events.

Our model estimates that, currently, oysters can decrease both Ω_{CA} and Ω_{AR} in the Damariscotta's growing area by approximately 3% each over the growing season. Although these changes are small, they may be important in systems with high DIC/TA ratios, such as the Damariscotta River Estuary, where ambient Ω_{CA} and Ω_{AR} remain close to 3 and 2, respectively, during the growing season. The same amount of oyster growth will drive this system closer to dissolution (Ω < 1) than in a more southern estuary with lower DIC/TA ratios (Morris and Humphreys, 2019). Any further reductions in TA and Ω require that oysters use more energy to create new shell (Melzner et al., 2011). Although juvenile and adult bivalves continue calcifying when Ω_{AR} is undersaturated, their calcification rate decreases (Gazeau et al., 2007; Miller et al., 2009; Ries et al., 2009; Waldbusser et al., 2010; Melzner et al., 2011). Schwaner et al. (2020) showed that larval and juvenile bivalves raised under high pCO₂, low pH treatments (pCO_2 approximately 1166 ppm, pH = 7.57) had increased susceptibility to disease and increased mortality, and Lord and Whitlatch (2014) showed that the thickness of eastern oyster shells is strongly tied to temperature (i.e., lower temperature increases pCO_2 and reduces Ω). If shell

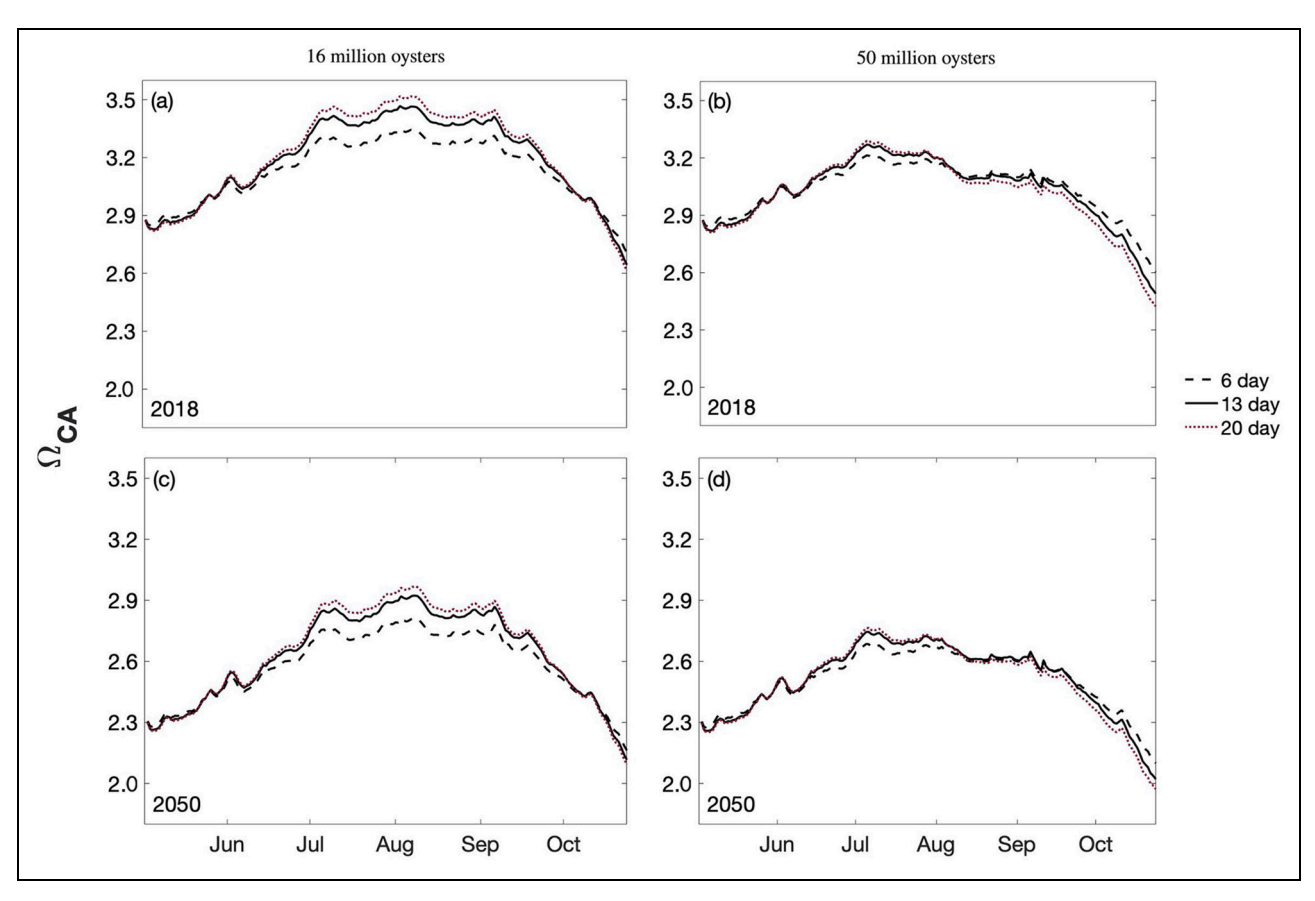


Figure 8. Impact of residence time on Ω_{CA} **in 2018 and 2050**. Modeled values of Ω_{CA} with (a) 2018 oceanic conditions and industry expansion, (c) 2050 oceanic conditions and no industry expansion, and (d) 2050 oceanic conditions and industry expansion. DOI: https://doi.org/10.1525/elementa.2020.00057.f8

thickness and/or hardness are reduced (Beniash et al., 2010; Meng et al., 2018), bivalves are expected to be more susceptible to predators, such as oyster drills, and may also be less valuable to the half shell market (Mizuta and Wikfors, 2019). First-year "seed" oysters are placed on the farm in the beginning of the growing season when Ω is low due to cold temperatures. The combination of low temperatures and reductions in Ω from oyster growth may lead to lower biomineralization rates by the juvenile oysters leading to increased mortality, particularly at higher industry sizes or future OCA conditions where Ω_{AR} approaches 1. Thus, understanding how cultured oysters and physical processes alter carbonate chemistry in tandem is important to inform sustainable growth of the industry and maintain a high-quality product.

Physical controls on Ω in this system are as important as oyster growth at the current industry size but can increase and decrease Ω and can be hard to predict. Higher temperatures from climate change will increase Ω due to its thermodynamic properties; however, increased atmospheric and in situ CO_2 concentrations from climate change will decrease Ω . Consistent with other models (Siedlecki et al., 2021), our model predicts that increasing in situ pCO_2 to levels projected for the Gulf of Maine will have a larger impact than increased temperature on Ω , leading to an overall decrease in Ω in the growing area. Our model predicts similar change in Ω (19% with zero

oysters present) to models used in Siedlecki et al. (2021), which predicted on average a 22% reduction in Ω during the growing season.

The inclusion of residence time, or oceanic exchange, in our model (Figure 3) was important, as it replenished TA lost to calcification under all scenarios. However, depending on the DIC, the oceanic exchange term either added more DIC or diluted the DIC pool. For scenarios modeled with 16 million oysters, between June and September, the DIC/TA ratio of the incoming ocean water was higher than that in the growing area (**Figure 8a** and **c**) because elevated temperatures in the growing area increased CO2 flux to the atmosphere. However, during May and October in the scenarios with 16 million oysters, or during the second half of the growing season with 50 million oysters and 2018 climate conditions, the incoming water had a lower DIC/TA ratio than the growing area, and reduced the overall DIC, increasing Ω . Thus, the impact of residence time was dependent on the seasonal temperature change and associated air-sea exchange, as well as the increase in oyster growth over the season.

Changes in residence time due to climate change may alter the impacts on Ω in several ways. If freshwater flow were included in the model, increased precipitation to the estuary and watershed would decrease the residence time (Scavia et al., 2002), but also likely lower the TA due to the higher DIC/TA ratio of freshwater, leading to lower Ω . A

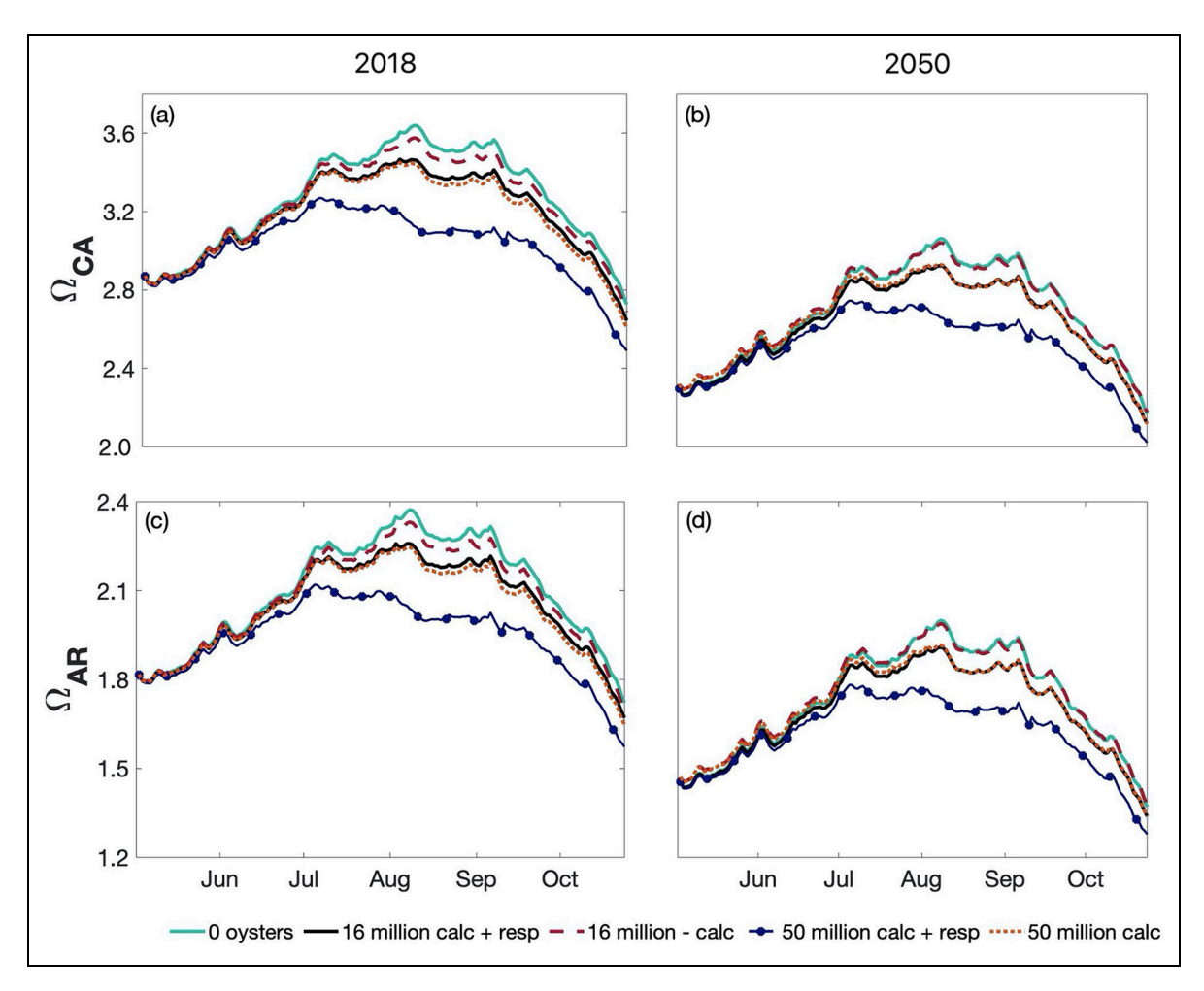


Figure 9. The impact of modeling only calcification vs calcification and respiration on Ω . Modeled (a, b) Ω_{CA} and (c, d) Ω_{AR} using zero oysters, 16 million oysters with calcification (calc) and respiration (resp) or calcification only, and 50 million oysters with calcification and respiration or calcification only for both 2018 (left) and 2050 (right). Temperature change, air-sea exchange, and oceanic exchange were included in all scenarios. Residence time = 13 days. DOI: https://doi.org/10.1525/elementa.2020.00057.f9

decrease in residence time due to sea-level rise (Du et al., 2018) would lessen the impact from oysters via increased volume exchange. However, it would also decrease Ω by lowering temperature and thus loss of CO_2 to the atmosphere, especially because the incoming water has a higher DIC/TA ratio than water in the growing area. Given the varied, often competing direct (mixing) and indirect (temperature-induced changes in air-water exchange) effects of altered residence time on Ω , more dynamic model simulations are desirable in the future.

Shellfish are just one part of complicated biogeochemical cycles in estuaries that can affect carbonate chemistry. The ratio of local primary production to calcification in various calcifying systems can control in situ *p*CO₂ (Suzuki, 1998), and therefore acidification. The impact of photosynthesis and respiration in this system does impact carbonate chemistry on short time scales (days—weeks, unpublished data), but averaged over the growing season, the growing area is slightly heterotrophic (–3.7 mmol O₂ m⁻² day⁻¹; Figure S2), which may indicate that photosynthesis is not able to capture all of the excess DIC released from oysters. As such, the current impact from oysters in

this system is likely somewhere between the calcificationonly and calcification-plus-respiration scenarios depicted in **Figure 9**. However, if the balance between photosynthesis and respiration in the growing area changes due to warming, altered watershed inputs, enhanced oyster grazing, or nutrient limitation, the impact of oyster respiration on Ω may change.

Carrying capacity, from a production perspective, is commonly defined as the maximum number of individuals that a given environment can sustain (Byron et al., 2011; Filgueira et al., 2015). Ecological carrying capacity seeks to balance production with minimal harm to the environment, to preserve pelagic and benthic habitats, and to maintain ecosystem functions (Byron et al., 2011; McKindsey, 2012). Ecological carrying capacity models lag behind production-based shellfish models, and most to date have focused on phytoplankton supply (Byron et al., 2011; Filgueira et al., 2014) or the impacts of biodeposition on benthic habitats (Grant and Filgueira, 2011). The effect of aquaculture on ambient carbonate chemistry has not previously been considered when establishing carrying capacity criteria (McKindsey, 2012;

Filgueira et al., 2015; Smaal and van Duren, 2019); however, our model results suggest that oyster aquaculture could impose limits on production or sustainable industry growth due to autoacidification, especially in low alkalinity ecosystems and very high industry sizes. In addition to the domain of our model, future carbonate carrying capacity models may need to incorporate sediment sources of acidity and alkalinity as increased biodeposition alters estuarine respiratory pathways (Thomas et al., 2009; Hu and Cai, 2011). To strike a balance between oyster production and ecosystem integrity, considering the impact of the shellfish aquaculture industry on the carbonate system may be important when developing future carrying capacity criteria, but almost certainly only in areas with Ω currently close to dissolution levels.

Conclusions

Our idealized model simulations suggest that cultured oysters have the ability to alter their surrounding carbonate chemistry through calcification and respiration, where the number of oysters is important in controlling the extent of Ω reduction through TA removal and DIC addition. Physical processes are important in controlling Ω , but the effects of air-sea gas and oceanic exchange depend strongly on the internal dynamics of DIC and TA production and consumption. The combination of future OCA conditions and future industry size will be important determinants of carrying capacity estimates. As shellfish aquaculture continues to expand worldwide, the need to consider not only how local and regional ocean acidification may affect growth of the species but also how shellfish growth itself, when at high densities, may impact the local carbonate budget is clear. An increasing number of biogeochemical models include some variables of the carbonate system, including calcification and dissolution (Shen et al., 2019; Gomez et al., 2020); however, depending on the resolution of the model, they may not capture localized impacts of shellfish aquaculture, and these local conditions are often important when predicting future growth rates and determining an ecological carrying capacity. We suggest that biogeochemical models of areas with emerging or sustained shellfish aquaculture industries include local growth rates and number of shellfish as part of the carbonate cycling variables to increase processlevel understanding and, ultimately, predictive capacity.

Data accessibility statement

Data from the LOBO buoy are accessible at: http://maine.loboviz.com/loboviz/.

Supplemental files

The supplemental files for this article can be found as follows:

Text S1. Figure S1–2. Docx

Acknowledgments

The authors thank Cheyenne Adams and Alwyn Ecker for their contribution of oyster shell height data, Kathleen Thornton for her guidance in laboratory methods, and Jon Lewis for his inquiry which inspired this project. They also thank the 3 reviewers who gave encouraging and constructive feedback to this manuscript. This is the University of Maryland Center for Environmental Science Publication No. 6058 and CBL Technical Series CBL 2022-018.

Funding

This activity was partially supported by the National Science Foundation award #IIA-1355457 to Maine EPSCoR and National Sea Grant (NA18OAR4170330) at the University of Maine (DC Brady, LM Mayer, and CM Liberti), by a NOAA Regional Vulnerability Assessments for Ocean Acidification award (DC Brady, LM Mayer), and by the United States National Oceanographic and Atmospheric Administration Ocean Acidification Program (NOAA-OAP; award # NA15NOS4780184 and NA18NOS4780179) to the University of Maryland Center for Environmental Science (JM Testa).

Competing interests

The authors have declared that no competing interests exist.

Author contributions

Contributed to conception and design: CML, MWG, DCB, LMM, JMT, WL.

Contributed to acquisition of data: CML, MWG.

Contributed to analysis and interpretation of data: CML, MWG, DCB, LMM, WL.

Drafted and/or revised the article: CML, MWG, DCB, LMM, JMT, WL.

Approved the submitted version for publication: CML, MWG, DCB, LMM, JMT, WL.

References

Adams, CM, Mayer, LM, Rawson, P, Brady, DC, Newell, C. 2019. Detrital protein contributes to oyster nutrition and growth in the Damariscotta Estuary, Maine, USA. *Aquaculture Environment Interactions* 11: 521–536. DOI: http://dx.doi.org/10.3354/aei00330.

Ahmed, N, Bunting, SW, Glaser, M, Flaherty, MS, Diana, JS. 2017. Can greening of aquaculture sequester blue carbon? *Ambio* **46**(4): 468–477. DOI: http://dx.doi.org/10.1007/s13280-016-0849-7.

Beniash, E, Ivanina, A, Lieb, N, Kurochkin, I, Sokolova, I. 2010. Elevated level of carbon dioxide affects metabolism and shell formation in oysters *Crassostrea virginica*. *Marine Ecology Progress Series* **419**: 95–108. DOI: http://dx.doi.org/10.3354/meps08841.

Brickman, D, Alexander, MA, Pershing, A, Scott, JD, Wang, Z. 2021. Projections of physical conditions in the Gulf of Maine in 2050. *Elementa Science of the Anthropocene* **9**(00055). DOI: http://dx.doi.org/10. 1525/elementa.2020.20.00055.

Byron, C, Link, J, Costa-Pierce, B, Bengtson, D. 2011. Calculating ecological carrying capacity of shellfish aquaculture using mass-balance modeling: Narragansett Bay, Rhode Island. *Ecological Modelling*

- **222**(10): 1743–1755. DOI: http://dx.doi.org/10. 1016/j.ecolmodel.2011.03.010.
- Cai, W-J, Huang, W-J, Luther, GW, Pierrot, D, Li, M, Testa, J, Xue, M, Joesoef, A, Mann, R, Brodeur, J, Xu, Y, Chen, B, Hussain, N, Waldbusser, GG, Cornwall, J, Kemp, MW. 2017. Redox reactions and weak buffering capacity lead to acidification in the Chesapeake Bay. *Nature Communications* 8(1): 1–12. Nature Publishing Group. DOI: http://dx.doi.org/10.1038/s41467-017-00417-7.
- Coen, LD, Dumbauld, BR, Judge, ML. 2011. Expanding shellfish aquaculture: A review of the ecological services provided by and impacts of native and cultured bivalves in shellfish-dominated ecosystems, in *Shell-fish aquaculture and the environment*. 1st ed. John Wiley & Sons, Inc.: 239–295. DOI: http://dx.doi.org/10.1002/9780470960967.ch9.
- **Cranford, PJ, Ward, JE, Shumway, SE.** 2011. Bivalve filter feeding: Variability and limits of the aquaculture biofilter, in Shumway, SE ed., *Shellfish aquaculture and the environment*. 1st ed. West Sussex, UK: John Wiley & Sons, Inc.: 81–124.
- **Dame, RF.** 2011. *Ecology of marine bivalves: An ecosystem approach, second edition.* Boca Raton, FL: CRC Press.
- **Dickson, AG.** 1981. An exact definition of total alkalinity and a procedure for the estimation of alkalinity and total inorganic carbon from titration data. *Deep Sea Research Part A. Oceanographic Research Papers* **28**(6): 609–623. DOI: http://dx.doi.org/10.1016/0198-0149(81)90121-7.
- **Dickson, AG, Millero, FJ.** 1987. A comparison of the equilibrium constants for the dissociation of carbonic acid in seawater media. *Deep Sea Research Part A. Oceanographic Research Papers* **34**(10): 1733–1743. DOI: http://dx.doi.org/10.1016/0198-0149(87)90021-5.
- **Dickson, AG, Sabine, CL, Christian, JR.** 2007. *Guide to best practices for ocean CO₂ measurements*. North Pacific Marine Science Organization. Available at https://repository.oceanbestpractices.org/handle/11329/249.
- Dickson, AG, Wesolowski, DJ, Palmer, DA, Mesmer, RE. 1990. Dissociation constant of bisulfate ion in aqueous sodium chloride solutions to 250°C. *Journal of Physical Chemistry* **94**(20): 7978–7985. DOI: http://dx.doi.org/10.1021/j100383a042
- Doney, SC, Fabry, VJ, Feely, RA, Kleypas, JA. 2009. Ocean acidification: The other CO₂ problem. *Annual Review of Marine Science* 1: 169–192. DOI: http://dx.doi.org/10.1146/annurev.marine.010908.163834.
- Du, J, Shen, J, Zhang, YJ, Ye, F, Liu, Z, Wang, Z, Wang, YP, Yu, X, Sisson, M, Wang, HV. 2018. Tidal response to sea-level rise in different types of estuaries: The importance of length, bathymetry, and geometry. *Geophysical Research Letters* **45**(1): 227–235. DOI: http://dx.doi.org/10.1002/2017GL075963.
- Duarte, CM, Hendriks, IE, Moore, TS, Olsen, YS, Steckbauer, A, Ramajo, L, Carstensen, J, Trotter, JA, McCulloch, M. 2013. Is ocean acidification an open-ocean syndrome? Understanding anthropogenic impacts on seawater pH. Estuaries and Coasts

- **36**(2): 221–236. DOI: http://dx.doi.org/10.1007/s12237-013-9594-3.
- **Dumbauld, BR, Ruesink, JL, Rumrill, SS.** 2009. The ecological role of bivalve shellfish aquaculture in the estuarine environment: A review with application to oyster and clam culture in West Coast (USA) estuaries. *Aquaculture* **290**(3): 196–223. DOI: http://dx.doi.org/10.1016/j.aquaculture.2009.02.033.
- Ekstrom, JA, Suatoni, L, Cooley, SR, Pendleton, LH, Waldbusser, GG, Cinner, JE, Ritter, J, Langdon, C, van Hooidonk, R, Gledhill, D, Wellman, K, Beck, MW, Brander, LM, Ritschof, D, Doherty, C, Edwardsw, PET, Portela, R. 2015. Vulnerability and adaptation of US shellfisheries to ocean acidification. *Nature Climate Change* 5(3): 207–214. DOI: http://dx.doi.org/10.1038/nclimate2508.
- **Enquist, BJ, Economo, EP, Huxman, TE, Allen, AP, Ignace, DD, Gillooly, JF.** 2003. Scaling metabolism from organisms to ecosystems. *Nature* **423**(6940): 639–642. DOI: http://dx.doi.org/10.1038/nature01671.
- Feely, RA, Alin, SR, Newton, J, Sabine, CL, Warner, M, Devol, A, Krembs, C, Maloy, C. 2010. The combined effects of ocean acidification, mixing, and respiration on pH and carbonate saturation in an urbanized estuary. *Estuarine, Coastal and Shelf Science* **88**(4): 442–449. DOI: http://dx.doi.org/10.1016/j.ecss.2010.05.004.
- Feely, RA, Sabine, CL, Hernandez-Ayon, JM, Ianson, D, Hales, B. 2008. Evidence for upwelling of corrosive "acidified" water onto the continental shelf. *Science* **320**(5882): 1490–1492. DOI: http://dx.doi.org/10. 1126/science.1155676.
- Feely, RA, Sabine, CL, Lee, K, Berelson, W, Kleypas, J, Fabry, VJ, Millero, FJ. 2004. Impact of anthropogenic CO₂ on the CaCO₃ system in the oceans. *Science* **305**(5682): 362–366.
- **Filgueira, R, Comeau, LA, Guyondet, T, McKindsey, CW, Byron, CJ.** 2015. Modelling carrying capacity of bivalve aquaculture: A review of definitions and methods, in Meyers, RA ed., *Encyclopedia of sustainability science and technology.* New York, NY: Springer: 1–33. DOI: http://dx.doi.org/10.1007/978-1-4939-2493-6_945-1.
- **Filgueira, R, Guyondet, T, Comeau, LA, Grant, J.** 2014. A fully-spatial ecosystem-DEB model of oyster (*Crassostrea virginica*) carrying capacity in the Richibucto Estuary, Eastern Canada. *Journal of Marine Systems* **136**: 42–54. DOI: http://dx.doi.org/10.1016/j.jmarsys.2014.03.015.
- Fodrie, FJ, Rodriguez, AB, Gittman, RK, Grabowski, JH, Lindquist, NL, Peterson, CH, Piehler, MF, Ridge, JT. 2017. Oyster reefs as carbon sources and sinks. *Proceedings of the Royal Society B Biological Sciences* **284**(1859): 20170891. DOI: http://dx.doi.org/10. 1098/rspb.2017.0891.
- Frankignoulle, M, Pichon, M, Gattuso, J-P. 1995. Aquatic calcification as a source of carbon dioxide, in Beran, MA ed., *Carbon sequestration in the*

- *biosphere.* Berlin, Heidelberg: Springer: 265–271. DOI: http://dx.doi.org/10.1007/978-3-642-79943-3_18.
- Friedland, KD, Morse, RE, Manning, JP, Melrose, DC, Miles, T, Goode, AG, Brady, DC, Kohut, JT, Powell, EN. 2020a. Trends and change points in surface and bottom thermal environments of the US Northeast continental shelf ecosystem. *Fisheries Oceanography* **29**(5): 396–414. DOI: http://dx.doi.org/10.1111/fog.12485.
- Friedland, KD, Morse, RE, Shackell, N, Tam, JC, Morano, JL, Moisan, JR, Brady, DC. 2020b. Changing physical conditions and lower and upper trophic level responses on the US Northeast Shelf. *Frontiers in Marine Science* 7. Frontiers. DOI: http://dx.doi.org/10.3389/fmars.2020.567445.
- Gattuso, J-P, Allemand, D, Frankignoulle, M. 1999. Photosynthesis and calcification at cellular, organismal and community levels in coral reefs: A review on interactions and control by carbonate chemistry. *Integrative and Comparative Biology* **39**(1): 160–183. DOI: http://dx.doi.org/10.1093/icb/39.1. 160
- Gattuso, J-P, Epitalon, J-M, Lavigne, H, Orr, JC, Gentili, B, Hagens, M, Hofmann, AF, Mueller, J-D, Proye, A, Rae, J, Soetaert, K. 2020. Seacarb: Seawater carbonate chemistry. Available at https://CRAN.R-project.org/package=seacarb.
- **Gattuso, J-P, Pichon, M, Frankignoulle, M**. 1995. Biological control of air-sea CO₂ fluxes: Effect of photosynthetic and calcifying marine organisms and ecosystems. *Marine Ecology Progress Series* **129**: 307–312. DOI: http://dx.doi.org/10.3354/meps129307.
- Gazeau, F, Parker, LM, Comeau, S, Gattuso, J-P, O'Connor, WA, Martin, S, Pörtner, H-O, Ross, PM. 2013. Impacts of ocean acidification on marine shelled molluscs. *Marine Biology* **160**(8): 2207–2245. DOI: http://dx.doi.org/10.1007/s00227-013-2219-3.
- **Gazeau, F, Quiblier, C, Jansen, JM, Gattuso, J-P, Middelburg, JJ, Heip, CHR.** 2007. Impact of elevated CO₂ on shellfish calcification. *Geophysical Research Letters* **34**(7). DOI: http://dx.doi.org/10.1029/2006GL028554.
- Gehlen, M, Barciela, R, Bertino, L, Brasseur, P, Butenschön, M, Chai, F, Crise, A, Drillet, Y, Ford, D, Lavoie, D, Lehodey, P, Parruche, C, Samuelsen, A, Simon, E. 2015. Building the capacity for forecasting marine biogeochemistry and ecosystems: Recent advances and future developments. *Journal of Operational Oceanography* 8(sup1): s168–s187. DOI: http://dx.doi.org/10.1080/1755876X.2015. 1022350.
- Gillikin, DP, Lorrain, A, Bouillon, S, Willenz, P, Dehairs, F. 2006. Stable carbon isotopic composition of *Mytilus edulis* shells: Relation to metabolism, salinity, δ¹³C_{DIC} and phytoplankton. *Organic Geochemistry* **37**(10): 1371–1382. DOI: http://dx.doi.org/10.1016/j.orggeochem.2006.03.008.

- Gillikin, DP, Lorrain, A, Meng, L, Dehairs, F. 2007. A large metabolic carbon contribution to the δ^{13} C record in marine aragonitic bivalve shells. *Geochimica et Cosmochimica Acta* **71**(12): 2936–2946. DOI: http://dx.doi.org/10.1016/j.gca.2007.04.003.
- Gledhill, DK, White, MM, Salisbury, JE, Thomas, H, MIsna, I, Liebman, M, Mook, B, Grear, JS, Candelmo, AC, Chambers, RC. 2015. Ocean and coastal acidification off New England and Nova Scotia. *Oceanography* 182–197. DOI: http://dx.doi.org/http://dx.doi.org/10.5670/oceanog.2015.41.
- Gomez, FA, Wanninkhof, R, Barbero, L, Lee, S-K, Hernandez, FJ. 2020. Seasonal patterns of surface inorganic carbon system variables in the Gulf of Mexico inferred from a regional high-resolution ocean biogeochemical model. *Biogeosciences* 17(6): 1685–1700. DOI: http://dx.doi.org/10.5194/bg-17-1685-2020.
- Gonçalves Neto, A, Langan, JA, Palter, JB. 2021. Changes in the Gulf Stream preceded rapid warming of the Northwest Atlantic Shelf. *Communications Earth and Environment* **2**(1): 1–10. DOI: http://dx.doi.org/10.1038/s43247-021-00143-5.
- **Grant, J, Filgueira, R**. 2011. The application of dynamic modeling to prediction of production carrying capacity in shellfish farming, in Shumway, SE ed., *Shellfish aquaculture and the environment*. 1st ed. West Sussex, UK: John Wiley & Sons, Inc.: 135–154.
- Hauri, C, Gruber, N, Plattner, G-K, Alin, SR, Feely, RA, Hales, B, Wheeler, PA. 2009. Ocean acidification in the California Current System. *Oceanography* 22(4): 60–71.
- Hauri, C, Gruber, N, Vogt, M, Doney, SC, Feely, RA, Lachkar, Z, Leinweber, A, McDonnell, AMP, Munnich, M, Plattner, G-K. 2013. Spatiotemporal variability and long-term trends of ocean acidification in the California Current System. *Biogeosciences* 10(1): 193–216. DOI: http://dx.doi.org/10.5194/bg-10-193-2013.
- **Hu, X, Cai, W-J.** 2011. An assessment of ocean margin anaerobic processes on oceanic alkalinity budget. *Global Biogeochemical Cycles* **25**(3). DOI: http://dx.doi.org/10.1029/2010GB003859.
- IPCC. 2014. Climate change 2014: Synthesis report. [Core writing team, Pachauri, RK, Meyer, LA, eds.] Contribution of WORKING Groups I, II and III to the Fifth Assessment Report of the Intergovernmental Panel on Climate Change. Geneva, Switzerland: IPCC: 151. IPCC. Report No.: 5.
- Jannasch, HW, Coletti, LJ, Johnson, KS, Fitzwater, SE, Needoba, JA, Plant, JN. 2008. The Land/Ocean Biogeochemical Observatory: A robust networked mooring system for continuously monitoring complex biogeochemical cycles in estuaries. *Limnology* and Oceanography Methods 6(7): 263–276. DOI: http://dx.doi.org/10.4319/lom.2008.6.263.
- Johnson, TR, Beard, K, Brady, DC, Byron, CJ, Cleaver, C, Duffy, K, Keeney, N, Kimble, M, Miller, M, Moeykens, S, Teisl, M, van Walsum, GP, Yuan, J. 2019. A social-ecological system framework for marine

- aquaculture research. *Sustainability* **11**(9): 2522. DOI: http://dx.doi.org/10.3390/su11092522.
- Kellogg, ML, Cornwell, JC, Owens, MS, Paynter, KT. 2013. Denitrification and nutrient assimilation on a restored oyster reef. *Marine Ecology Progress Series* 480: 1–19. DOI: http://dx.doi.org/10.3354/ meps10331.
- Kellogg, ML, Smyth, AR, Luckenbach, MW, Carmichael, RH, Brown, BL, Cornwell, JC, Piehler, MF, Owens, MS, Dalrymple, DJ, Higgins, CB. 2014. Use of oysters to mitigate eutrophication in coastal waters. *Estuarine, Coastal and Shelf Science* **151**: 156–168. DOI: http://dx.doi.org/10.1016/j.ecss. 2014.09.025.
- **Lejart, M, Clavier, J, Chauvaud, L, Hily, C.** 2012. Respiration and calcification of *Crassostrea gigas*: Contribution of an intertidal invasive species to coastal ecosystem CO₂ Fluxes. *Estuaries and Coasts* **35**(2): 622–632. DOI: http://dx.doi.org/10.1007/s12237-011-9462-y.
- Li, J, Zhang, W, Ding, J, Xue, S, Huo, E, Ma, Z, Yu, W, Jiang, Z, Fang, J, Mao, Y. 2021. Effect of large-scale kelp and bivalve farming on seawater carbonate system variations in the semi-enclosed Sanggou Bay. *Science of the Total Environment* **753**: 142065. DOI: http://dx.doi.org/10.1016/j.scitotenv.2020.142065.
- **Lieberthal, B, Huguenard, K, Ross, L, Liu, Z.** 2019. Intratidal variability of water quality in the Damariscotta River, Maine. *Water* **11**(12): 2603. DOI: http://dx.doi.org/10.3390/w11122603.
- **Lord, J, Whitlatch, R.** 2014. Latitudinal patterns of shell thickness and metabolism in the eastern oyster *Crassostrea virginica* along the east coast of North America. *Marine Biology* **161**(7): 1487–1497. DOI: http://dx.doi.org/10.1007/s00227-014-2434-6.
- **Lorrain, A, Paulet, Y-M, Chauvaud, L, Dunbar, R, Mucciarone, D, Fontugne, M.** 2004. δ¹³C variation in scallop shells: Increasing metabolic carbon contribution with body size? *Geochimica et Cosmochimica Acta* **68**(17): 3509–3519. DOI: http://dx.doi.org/10.1016/j.gca.2004.01.025.
- **Lunstrum, A, McGlathery, K, Smyth, A.** 2018. Oyster (*Crassostrea virginica*) aquaculture shifts sediment nitrogen processes toward mineralization over denitrification. *Estuaries and Coasts* **41**(4): 1130–1146. DOI: http://dx.doi.org/10.1007/s12237-017-0327-x.
- Maine Department of Marine Resources. 2020. Harvest of farm-raised American oysters (*Crassostrea virginica*) in Maine. Available at https://www.maine.gov/dmr/aquaculture/harvestdata/documents/americanoyster2005-19.pdf.
- Maine Department of Marine Resources. 2021. Active LPA licenses per year: 2007–2020. Available at https://www.maine.gov/dmr/aquaculture/data/documents/ActiveLPAsPerYear2007-2020.pdf. Accessed 7 June 2021.
- Marie, B, Zanella-Cléon, I, Guichard, N, Becchi, M, Marin, F. 2011. Novel proteins from the calcifying shell matrix of the Pacific oyster *Crassostrea gigas*.

- *Marine Biotechnology* **13**(6): 1159–1168. DOI: http://dx.doi.org/10.1007/s10126-011-9379-2.
- Mayer, LM, Townsend, DW, Pettigrew, NR, Loder, TC, Wong, MW, Kistner-Morris, D, Laursen, AK, Schoudel, AD, Conairis, C, Brown, J, Newell, C. 1996. *The Kennebec, Sheepscot and Damariscotta River estuaries: Seasonal oceanographic data.* Orono, ME: University of Maine. Report No.: 9601.
- **McAlice, B.** 1977. A preliminary oceanographic survey of the Damariscotta River Estuary, Lincoln County, Maine. Orono, ME: University of Maine. Report No.: Maine Sea Grant TR-13-77.
- McConnaughey, TA, Burdett, J, Whelan, JF, Paull, CK. 1997. Carbon isotopes in biological carbonates: Respiration and photosynthesis. *Geochimica et Cosmochimica Acta* **61**(3): 611–622. DOI: http://dx.doi.org/10.1016/S0016-7037(96)00361-4.
- McGarry, K, Siedlecki, SA, Salisbury, J, Alin, SR. 2021. Multiple linear regression models for reconstructing and exploring processes controlling the carbonate system of the northeast US from basic hydrographic data. *Journal of Geophysical Research: Oceans* 126(2): e2020JC016480. DOI: http://dx.doi.org/10.1029/2020JC016480
- **McKindsey, CW.** 2012. Carrying capacity for sustainable bivalve aquaculture, in Meyers, RA ed., *Encyclopedia of sustainability science and technology.* New York, NY: Springer: 1959–1976. DOI: http://dx.doi.org/10.1007/978-1-4419-0851-3_179.
- Mehrbach, C, Culberson, CH, Hawley, JE, Pytkowicx, RM. 1973. Measurement of the apparent dissociation constants of carbonic acid in seawater at atmospheric pressure. *Limnology and Oceanography* **18**(6): 897–907. DOI: http://dx.doi.org/10.4319/lo.1973.18.6.0897.
- Melzner, F, Stange, P, Trübenbach, K, Thomsen, J, Casties, I, Panknin, U, Gorb, SN, Gutowska, MA. 2011. Food supply and seawater pCO₂ impact calcification and internal shell dissolution in the blue mussel *Mytilus edulis. PLoS One* **6**(9). DOI: http://dx.doi.org/10.1371/journal.pone.0024223.
- Meng, Y, Guo, Z, Fitzer, SC, Upadhyay, A, Chan, VBS, Li, C, Cusack, M, Yao, H, Yeung, KWK, Thiyagarajan, V. 2018. Ocean acidification reduces hardness and stiffness of the Portuguese oyster shell with impaired microstructure: A hierarchical analysis. *Biogeosciences* 15(22): 6833–6846. DOI: http://dx.doi.org/https://doi.org/10.5194/bg-15-6833-2018.
- Menne, MJ, Durre, I, Korzeniewski, B, McNeal, S, Thomas, K, Yin, X, Anthony, S, Ray, R, Vose, RS, Gleason, BE, Houston, TG. 2019. Global Historical Climatology Network–Daily (GHCN-Daily). NOAA National Climatic Data Center: Version 3.26. Available at http://dx.doi.org/10.7289/V5D21VHZ.
- Miller, AW, Reynolds, AC, Sobrino, C, Riedel, GF. 2009. Shellfish face uncertain future in high CO₂ world: Influence of acidification on oyster larvae calcification and growth in estuaries. *PLoS One* **4**(5): e5661. DOI: http://dx.doi.org/10.1371/journal.pone. 0005661.

- **Mistri, M, Munari, C.** 2012. Clam farming generates CO₂: A study case in the Marinetta lagoon (Italy). *Marine Pollution Bulletin* **64**(10): 2261–2264. DOI: http://dx.doi.org/10.1016/j.marpolbul.2012.07.010.
- **Mizuta, DD, Wikfors, GH.** 2019. Seeking the perfect oyster shell: A brief review of current knowledge. *Reviews in Aquaculture* **11**(3): 586–602. DOI: http://dx.doi.org/10.1111/raq.12247.
- Moataz, M. 2021. Sea water properties function. MATLAB Central File Exchange. Available at https://www.mathworks.com/matlabcentral/fileexchange/31210-sea-water-properties-function. Accessed 10 June 2021.
- Morris, JP, Humphreys, MP. 2019. Modelling seawater carbonate chemistry in shellfish aquaculture regions: Insights into CO₂ release associated with shell formation and growth. *Aquaculture* **501**: 338–344. DOI: http://dx.doi.org/10.1016/j.aquaculture.2018. 11.028.
- **Munari, C, Rossetti, E, Mistri, M.** 2013. Shell formation in cultivated bivalves cannot be part of carbon trading systems: A study case with *Mytilus galloprovincialis. Marine Environmental Research* **92**: 264–267. DOI: http://dx.doi.org/10.1016/j.marenvres.2013.10.006.
- Naylor, RL, Hardy, RW, Buschmann, AH, Bush, SR, Cao, L, Klinger, DH, Little, DC, Lubchenco, J, Shumway, SE, Troell, M. 2021. A 20-year retrospective review of global aquaculture. *Nature* **591**(7851): 551–563. DOI: http://dx.doi.org/10.1038/s41586-021-03308-6.
- Newell, CR, Hawkins, AJS, Morris, K, Boss, E, Thomas, AC, Kiffney, TJ, Brady, DC. 2021. Using high-resolution remote sensing to characterize suspended particulate organic matter as bivalve food for aquaculture site selection. *Journal of Shellfish Research* **40**(1): 113–118.
- NOAA Fisheries. 2021. U.S. Aquaculture | NOAA Fisheries. NOAA. Available at https://www.fisheries.noaa.gov/national/aquaculture/us-aquaculture. Accessed 7 June 2021.
- **O'Sullivan, DW, Millero, FJ.** 1998. Continual measurement of the total inorganic carbon in surface seawater. *Marine Chemistry* **60**(1): 75–83. DOI: http://dx.doi.org/10.1016/S0304-4203(97)00079-0.
- Pacella, SR, Brown, CA, Waldbusser, GG, Labiosa, RG, Hales, B. 2018. Seagrass habitat metabolism increases short-term extremes and long-term offset of CO₂ under future ocean acidification. *Proceedings of the National Academy of Sciences of the United States of America* 115(15): 3870–3875.
- **Ray, NE, Maguire, TJ, Al-Haj, AN, Henning, MC, Fulweiler, RW.** 2019. Low greenhouse gas emissions from oyster aquaculture. *Environmental Science and Technology* **53**(15): 9118–9127. DOI: http://dx.doi.org/10.1021/acs.est.9b02965.
- **Raymond, PA, Cole, JJ.** 2001. Gas exchange in rivers and estuaries: Choosing a gas transfer velocity. *Estuaries and Coasts* **24**(2): 312–317.
- Reum, JCP, Alin, SR, Harvey, CJ, Bednaršek, N, Evans, W, Feely, RA, Hales, B, Lucey, N, Mathis, JT,

- McElhany, P, Newton, J, Sabine, CL. 2016. Interpretation and design of ocean acidification experiments in upwelling systems in the context of carbonate chemistry co-variation with temperature and oxygen. *ICES Journal of Marine Science* **73**(3): 582–595. DOI: http://dx.doi.org/10.1093/icesjms/fsu231.
- Rheuban, JE, Doney, SC, McCorkle, DC, Jakuba, RW. 2019. Quantifying the effects of nutrient enrichment and freshwater mixing on coastal ocean acidification. *Journal of Geophysical Research: Oceans* 124(12): 9085–9100. DOI: http://dx.doi.org/10. 1029/2019JC015556.
- **Ries, JB, Cohen, AL, McCorkle, DC.** 2009. Marine calcifiers exhibit mixed responses to CO₂-induced ocean acidification. *Geology* **37**(12): 1131–1134.
- Salisbury, J, Green, M, Hunt, CW, Campbell, J. 2008. Coastal acidification by rivers: A threat to shellfish? Eos Transactions American Geophysical Union 89(50): 513.
- **Salisbury, JE, Jönsson, BF.** 2018. Rapid warming and salinity changes in the Gulf of Maine alter surface ocean carbonate parameters and hide ocean acidification. *Biogeochemistry* **141**(3): 401–418. DOI: http://dx.doi.org/10.1007/s10533-018-0505-3.
- Scavia, D, Field, JC, Boesch, DF, Buddemeier, RW, Burkett, V, Cayan, DR, Fogarty, M, Harwell, MA, Howarth, RW, Mason, C, Reed, DJ, Royer, TC, Sallenger, AH, Titus, JG. 2002. Climate change impacts on U.S. coastal and marine ecosystems. *Estuaries* 25(2): 149–164. DOI: http://dx.doi.org/10.1007/BF02691304.
- Schwaner, C, Barbosa, M, Connors, P, Park, T-J, de Silva, D, Griffith, A, Gobler, CJ, Pales, EE, Allam, B. 2020. Experimental acidification increases susceptibility of *Mercenaria mercenaria* to infection by *Vibrio* species. *Marine Environmental Research* 154: 104872. DOI: http://dx.doi.org/10.1016/j.marenvres. 2019.104872.
- **Shchepetkin, AF, McWilliams, JC.** 2005. The regional oceanic modeling system (ROMS): A split-explicit, free-surface, topography-following-coordinate oceanic model. *Ocean Modelling* **9**(4): 347–404. DOI: http://dx.doi.org/10.1016/j.ocemod.2004.08.002.
- Shen, C, Testa, JM, Li, M, Cai, W-J, Waldbusser, GG, Ni, W, Kemp, WM, Cornwell, J, Chen, B, Brodeur, J, Su, J. 2019. Controls on carbonate system dynamics in a coastal plain estuary: A modeling study. *Journal of Geophysical Research: Biogeosciences* 124(1): 61–78. DOI: http://dx.doi.org/10.1029/2018JG004802.
- Siedlecki, SA, Salisbury, J, Gledhill, DK, Bastidas, C, Meseck, S, McGarry, K, Hunt, CW, Alexander, M, Lavoie, D, Wang, ZA, Scott, J, Brady, DC, MIsna, I, Azetsu-Scott, K, Liberti, CM, Melrose, DC, White, MM, Pershing, A, Vandemark, D, Townsend, DW, Chen, C, Mook, W, Morrison, R. 2021. Projecting ocean acidification impacts for the Gulf of Maine to 2050: new tools and expectations. Elementa: Science of the Anthropocene 9(1). DOI: http://

- dx.doi.org/https://doi.org/10.1525/elementa. 2020.20.00062.
- Smaal, AC, van Duren, LA. 2019. Bivalve aquaculture carrying capacity: Concepts and assessment tools, in Smaal, AC, Ferreira, JG, Grant, J, Petersen, JK, Strand, Ø eds., *Goods and services of marine bivalves*. Cham, Switzerland: Springer International Publishing: 451–483. DOI: http://dx.doi.org/10.1007/978-3-319-96776-9_23.
- **Suzuki, A.** 1998. Combined effects of photosynthesis and calcification on the partial pressure of carbon dioxide in seawater. *Journal of Oceanography* **54**(1): 1–7. DOI: http://dx.doi.org/10.1007/BF02744376.
- The Hale Group, Ltd, Gulf of Maine Research Institute. 2016. Maine farmed shellfish market analysis. Available at https://www.gmri.org/sites/default/files/resource/gmri_farmed_shellfish_final_with_cover_10.13.16.pdf.
- Thomas, H, Schiettecatte, L-S, Suykens, K, M Kone, YJ, Shadwick, EH, F Prowe, AE, Bozec, Y, W de Baar, HJ, Borges, AV. 2009. Enhanced ocean carbon storage from anaerobic alkalinity generation in coastal sediments. *Biogeosciences* **6**: 267–274.
- **Uppström, LR.** 1974. The boron/chlorinity ratio of deepsea water from the Pacific Ocean. *Deep Sea Research and Oceanographic Abstracts* **21**(2): 161–162. DOI: http://dx.doi.org/10.1016/0011-7471(74)90074-6.
- van Heuven, S, Pierrot, D, Rae, JWB, Lewis, E, Wallace, DWR. 2011. *MATLAB program developed for CO₂ system*. Oak Ridge, TN: ORNL/CDIAC-105b. Carbon Dioxide Information Analysis Center, Oak Ridge National Laboratory, U.S. Department of Energy. Available at DOI: http://dx.doi.org/10.3334/CDIAC/otg.CO2SYS_MATLAB_v1.1.
- Waldbusser, GG, Bergschneider, H, Green, MA. 2010. Size-dependent pH effect on calcification in post-larval hard clam *Mercenaria* spp. *Marine Ecology Progress Series* 417: 171–182. DOI: http://dx.doi.org/10.3354/meps08809.

- Waldbusser, GG, Hales, B, Langdon, CJ, Haley, BA, Schrader, P, Brunner, EL, Gray, MW, Miller, CA, Gimenez, I. 2015. Saturation-state sensitivity of marine bivalve larvae to ocean acidification. *Nature Climate Change* 5(3): 273–280. DOI: http://dx.doi.org/10.1038/nclimate2479.
- **Waldbusser, GG, Powell, EN, Mann, R.** 2013. Ecosystem effects of shell aggregations and cycling in coastal waters: An example of Chesapeake Bay oyster reefs. *Ecology* **94**(4): 895–903. DOI: http://dx.doi.org/10. 1890/12-1179.1.
- Waldbusser, GG, Salisbury, JE. 2014. Ocean acidification in the coastal zone from an organism's perspective: Multiple system parameters, frequency domains, and habitats. *Annual Review of Marine Science* 6(1): 221–247. DOI: http://dx.doi.org/10.1146/ annurev-marine-121211-172238.
- Wallace, RB, Baumann, H, Grear, JS, Aller, RC, Gobler, CJ. 2014. Coastal ocean acidification: The other eutrophication problem. *Estuarine, Coastal and Shelf Science* **148**: 1–13.
- Wang, ZA, Wanninkhof, R, Cai, W-J, Byrne, RH, Hu, X, Peng, T-H, Huang, W-J. 2013. The marine inorganic carbon system along the Gulf of Mexico and Atlantic coasts of the United States: Insights from a transregional coastal carbon study. *Limnology and Oceanography* **58**(1): 325–342. DOI: http://dx.doi.org/10. 4319/lo.2013.58.1.0325.
- **Wanninkhof, R.** 2014. Relationship between wind speed and gas exchange over the ocean revisited. *Limnology and Oceanography Methods* **12**(6): 351–362. DOI: http://dx.doi.org/10.4319/lom.2014.12.351.
- Ware, JR, Smith, SV, Reaka-Kudla, ML. 1992. Coral reefs: Sources or sinks of atmospheric CO₂? *Coral Reefs* 11(3): 127–130. DOI: http://dx.doi.org/10. 1007/BF00255465.
- **Zeebe, RE, Wolf-Gladrow, D**. 2001. *CO*₂ in seawater: Equilibrium, kinetics, isotopes. Amsterdam, the Netherlands: Gulf Professional Publishing.

How to cite this article: Liberti, CM, Gray, MW, Mayer, LM, Testa, JM, Liu, W, Brady, DC. 2022. The impact of oyster aquaculture on the estuarine carbonate system. *Elementa: Science of the Anthropocene* 10(1). DOI: https://doi.org/10.1525/elementa.2020.00057

Domain Editor-in-Chief: Jody W. Deming, University of Washington, Seattle, WA, USA

Guest Editor: Andrew Pershing, Climate Central, Princeton, NJ, USA

Knowledge Domain: Ocean Science

Part of an Elementa Special Feature: Gulf of Maine 2050: Visioning Regional Resilience and Sustainability

Published: January 7, 2022 Accepted: December 3, 2021 Submitted: May 23, 2020

Copyright: © 2022 The Author(s). This is an open-access article distributed under the terms of the Creative Commons Attribution 4.0 International License (CC-BY 4.0), which permits unrestricted use, distribution, and reproduction in any medium, provided the original author and source are credited. See http://creativecommons.org/licenses/by/4.0/.

